batteries

Review

A Comprehensive Review of Multiple Physical and Data-Driven Model Fusion Methods for Accurate Lithium-Ion Battery Inner State Factor Estimation

Junjie Tao [1], Shunli Wang [1,2,*], Wen Cao [1], Carlos Fernandez [3] and Frede Blaabjerg [4]

[1] School of Information Engineering, Southwest University of Science and Technology, Mianyang 621010, China; 7220230426@mails.swust.edu.cn (J.T.); caowen@swust.edu.cn (W.C.)
[2] Electric Power College, Inner Mongolia University of Technology, Hohhot 010021, China
[3] School of Pharmacy and Life Sciences, Robert Gordon University, Aberdeen AB10-7GJ, UK; c.fernandez@rgu.ac.uk
[4] Department of Energy Technology, Aalborg University, Pontoppidanstraede 111, 9220 Aalborg East, Denmark; fbl@energy.aau.dk
* Correspondence: wangshunli@imut.edu.cn

Abstract: With the rapid global growth in demand for renewable energy, the traditional energy structure is accelerating its transition to low-carbon, clean energy. Lithium-ion batteries, due to their high energy density, long cycle life, and high efficiency, have become a core technology driving this transformation. In lithium-ion battery energy storage systems, precise state estimation, such as state of charge, state of health, and state of power, is crucial for ensuring system safety, extending battery lifespan, and improving energy efficiency. Although physics-based state estimation techniques have matured, challenges remain regarding accuracy and robustness in complex environments. With the advancement of hardware computational capabilities, data-driven algorithms are increasingly applied in battery management, and multi-model fusion approaches have emerged as a research hotspot. This paper reviews the fusion application between physics-based and data-driven models in lithium-ion battery management, critically analyzes the advantages, limitations, and applicability of fusion models, and evaluates their effectiveness in improving state estimation accuracy and robustness. Furthermore, the paper discusses future directions for improvement in computational efficiency, model adaptability, and performance under complex operating conditions, aiming to provide theoretical support and practical guidance for developing lithium-ion battery management technologies.

Keywords: lithium-ion battery; state of charge estimation; physical modeling approach; data-driven approach; multi-model fusion approach

Citation: Tao, J.; Wang, S.; Cao, W.; Fernandez, C.; Blaabjerg, F. A Comprehensive Review of Multiple Physical and Data-Driven Model Fusion Methods for Accurate Lithium-Ion Battery Inner State Factor Estimation. *Batteries* **2024**, *10*, 442. https://doi.org/10.3390/batteries10120442

Academic Editor: Pascal Venet

Received: 14 November 2024
Revised: 2 December 2024
Accepted: 12 December 2024
Published: 13 December 2024

1. Introduction

Many countries worldwide vigorously promote carbon neutrality and the goal of carbon peaking. Lithium-ion batteries (LIB) play a key role in this process, especially in the wide application of electric vehicles and energy storage systems [1]. Accurate battery state estimation is essential to realizing energy savings and efficiency, extending battery life, and improving the economy of new energy vehicles and energy storage systems [2].

The state estimation of lithium-ion batteries mainly includes the estimation of parameters such as state of charge (SOC) [3], state of health (SOH) [4], and state of power (SOP) [5]. Currently, the development of state estimation techniques can be summarized into three main categories: model-based [6], data-driven [7], and hybrid methods [8]. Model-based methods were the first to be applied to battery state estimation by building the electrochemical model (EM) [9] or equivalent circuit model (ECM) [10] of the battery. For example, a common algorithm combining ECM and extended Kalman filter (EKF) [11] uses EKF to perform state estimation on a battery state space model constructed by ECM. Or the combination of EM and particle filter (PF) [12], which first captures the internal chemical

kinetic processes of the battery by EM and then performs nonlinear state estimation by PF. They are all physical model-based algorithms with good interpretability, strong generalization, and high real-time performance [13]. However, they also have strong parameter dependence, high computational complexity, and sensitivity to noise and errors [14]. Unlike physical model-based estimation methods, data-driven methods do not rely on the physical characteristics or ECM of the battery but instead perform state estimation by extracting features and patterns from historical data [15]. Common machine learning algorithms include support vector machine (SVM) [16], random forest (RF) [17], gradient boosting decision tree (GBDT) [18], extreme learning machine (ELM) [19], etc.; common deep learning algorithms include convolutional neural networks (CNN) [20], long short-term memory (LSTM) neural networks [21], deep neural networks (DNN) [22], and autoencoder [23]. Machine learning algorithms are easy to implement, have low computational overhead, and are suitable for small datasets [24]. However, they have a high reliance on feature engineering, and it is difficult to handle complex nonlinear problems [25]. Deep learning algorithms are suitable for scenarios with large-scale data, nonlinear complex relationships, and time series processing [26]. However, they consume large computational resources, have a long training time, and lack model interpretability [27].

The hybrid approach combines model-based physical or electrochemical methods with data-driven machine learning or deep learning algorithms [28]. It leverages the interpretability and reliability of physical models' prior knowledge while exploiting the capability of data-driven models to handle complex nonlinear relationships. This hybrid approach is the main focus of this paper, and the following are common combination strategies: (a) The physical model generates preliminary predictions, corrected by a data-driven model. In this approach, different algorithms are generally connected in series. A physical model, such as an ECM or EM, first provides an initial estimate of the battery state, while the data-driven model corrects errors in the physical model to improve prediction accuracy. Zhang et al. [29] proposed a real-time LIB soft fault detection framework that combines a physical model observer and bidirectional LSTM (Bi-LSTM). Initially, the ECM coupled thermal model and the EKF monitor the battery voltage and surface temperature to provide a fundamental estimate of the battery state. Then, a Bi-LSTM-based learning method is employed to model and compensate for uncertainties in these residuals. The optimized residual signal obtained is used to identify battery fault information, enabling soft short-circuit fault detection by setting safety thresholds. (b) The data-driven model extracts complex features constrained and interpreted by the physical model. Here, the data-driven model automatically extracts complex features from large datasets, while the physical model imposes certain boundary conditions or constraints, ensuring the model's predictions are physically reasonable, thus avoiding overfitting and bias. Meng et al. [30] introduced a Bayesian neural network (BNN) model integrating physical knowledge and data-driven approaches, using a fault tree to model physical knowledge, complemented by data-driven methods learned from accident data to construct an expert-knowledge-based BNN. Additionally, they employed a Bow-tie model to embed safety barriers (e.g., detectors, emergency responses, and fire suppression facilities) into the BNN for risk control and evaluation. The verification demonstrates that these measures significantly reduce accident risks. (c) Joint optimization of model parameters. Physical models often rely on certain parameters for accurate state estimation, yet these parameters frequently change with battery aging. By using data-driven models to learn the patterns of parameter variations and adjust the physical model parameters online, the accuracy of the physical model under different operating conditions and states can be enhanced. Nicodemo et al. [31] proposed a method to predict key parameters of the pseudo-two-dimensional model (P2D) model from ECM parameters using neural network (NN). First, the P2D model generates a synthetic dataset to simulate battery behavior under different aging stages. Relevant ECM parameters are then extracted from this simulated data to train the NN. The NN inputs include multiple resistance and capacitance parameters at different SOC levels, while the outputs are five electrochemical parameters in the P2D model, characterizing lithium-ion

diffusion within electrodes and reaction kinetics at the electrode interface. (d) Parallel prediction at the model level. The physical and data-driven models operate simultaneously, and their prediction results are integrated through a fusion mechanism (e.g., weighted averaging or KF) to yield a more accurate state estimation. Zhang et al. [32] proposed a data-driven multi-model fusion method for SOH estimation of LIB. All possible operating conditions are categorized into six scenarios, each with a specific set of features. Gaussian process regression (GPR), Bayesian ridge regression (BRR), random forest regression (RFR), and DNN, four machine learning algorithms, are employed to provide SOH estimates at the current moment, along with quantifying the confidence interval of each estimate. Finally, KF is introduced to fuse these estimations. This multi-model fusion approach enhances estimation accuracy and enables real-time integration of historical data.

In recent years, scholars have systematically summarized and analyzed the current research status, challenges, and future trends in LIB state estimation from various perspectives, including model-based algorithms, machine learning algorithms, and deep learning algorithms. Ji et al. [33] reviewed LIB modeling methods from two perspectives: mechanism-based and data-driven models. The article first revisits existing mechanism-based physical models, including ECM and P2D models, and explores the impact of electrode morphology and aging-related side reactions on battery performance. Following this, the authors also provide a detailed introduction to various data-driven models used for battery SOH estimation through machine learning and, further, discuss the potential of combining mechanism models with data-driven models. Zhao et al. [34] reviewed different prediction methods for LIB state estimation (SOC, SOH, and remaining useful life (RUL)), primarily covering experimental methods, model-based methods, data-driven methods, and hybrid methods, emphasizing their critical role in extending battery life and ensuring system reliability. The article first introduces the existing definitions and estimation methods for battery states, providing a detailed classification and comparison of each approach. Finally, the article summarizes the challenges in current research, noting that overcoming the limitations of individual methods by combining multiple approaches is an effective way to achieve a smarter and more reliable battery management system (BMS). From a control-oriented perspective, Ghaeminezhad et al. [35] systematically reviewed recent advances in SOC estimation for LIB, categorizing existing methods into open-loop, closed-loop, and hybrid approaches. The article discusses the advantages and disadvantages of each method in detail, with particular emphasis on the effectiveness of enhancing estimation accuracy and robustness through feedback control, such as using filters and observers. Additionally, the article presents various optimized and combined state estimation strategies, suggesting that future research in this field will focus on optimizing control strategies to achieve more efficient and lower-complexity BMS. Table 1 presents an overview of other literature reviews on LIB state estimation in recent years, summarizing their methods and key highlights.

Table 1. Literature review of lithium-ion battery state estimation.

Author	Years	Target Estimation States	Methods	Highlights
Zhou et al. [36]	2023	SOC	ECM-based, data-driven	Emphasizes the potential application of cutting-edge technologies in battery state estimation, such as intelligent sensing, big data, and cloud computing.
Tao et al. [37]	2024	SOC, SOH	ECM-based, EM-based, data-driven, hybrid models	Provides a comprehensive analysis of different types of algorithms, with an in-depth discussion on the critical role of datasets and future trends in state estimation.

Table 1. *Cont.*

Author	Years	Target Estimation States	Methods	Highlights
Liu et al. [38]	2023	SOH	ECM-based, data-driven	Systematically reviews the application of Electrochemical impedance spectroscopy (EIS) in SOH estimation for LIB.
Urquizo et al. [39]	2023	SOH	ECM-based, EM-based, empirical models, performance-based, statistical models	Discusses each model's advantages and disadvantages in detail, emphasizes the need for new testing standards and experimental data for battery energy systems, and summarizes the results of accelerated aging tests.
Liu et al. [40]	2023	SOC, SOH, SOP, State of energy (SOE), State of temperature (SOT)	ECM-based, data-driven	Systematically summarizes the definitions of seven major battery states and their interrelationships, highlighting the technical challenges and future directions for multi-state joint estimation.
Sun et al. [41]	2023	SOH	ECM-based, data-driven	Highlights the advantages of EIS as a non-destructive testing method and proposes a trend toward combining model-driven and data-driven approaches.
Ren et al. [42]	2023	SOC, SOH	Data-driven	Discusses the performance of different machine learning algorithms through numerous practical application cases from recent studies.
Martí-Florences et al. [43]	2023	SOC, SOH	ECM-based, EM-based, data-driven	Focuses on various EM simplification methods and provides an in-depth analysis of finite-dimensional simplification models, such as finite difference and finite volume methods.
Ouyang et al. [44]	2023	SOH, RUL	ECM-based, EM-based, empirical models, black-box models	Conducts a systematic review of battery aging mechanisms, model construction, and SOH estimation, integrating Bayesian methods with existing battery health management techniques.
Yang et al. [45]	2024	SOH	ECM-based, EM-based, data-driven	Systematically summarizes data-driven and hybrid methods, reviews commonly used public battery datasets and provides a forward-looking analysis of SOH estimation trends.

As shown in Table 1, recent reviews on LIB state estimation have primarily focused on model-based and data-driven algorithms, with only a few studies covering empirical models and other methods. The fusion of physical models and data-driven algorithms is widely regarded as a key direction for future research and technological development; however, a systematic synthesis and summary are still lacking. Therefore, this paper reviews recent representative state estimation algorithms from multi-physics model fusion and multi-data-driven fusion perspectives. Specifically, it systematically summarizes recent advancements in hybrid integrating multi-physics models and data-driven approaches, aiming to offer a reference for the field's future development.

The remaining structure of this paper is organized as follows: Section 2 provides detailed definitions of the main state parameters for LIBs and their methods of definition; Section 3 discusses state estimation algorithms based on multi-physics model fusion; Section 4 focuses on state estimation methods based on multi-data-driven fusion; Section 5 systematically summarizes hybrid fusion techniques that combine multi-physics models with data-driven approaches; Section 6 presents a comprehensive summary of the

study's content and main conclusions. Additionally, explanations for all abbreviations used throughout the text are listed in alphabetical order for reference, as shown in Table 2.

Table 2. Abbreviations and explanations of common nouns.

Abbreviations	Explanations	Abbreviations	Explanations
AEKF	Adaptive Extended Kalman Filter	MPC	Model Predictive Control
AR	Autoregressive	NARX	Nonlinear Autoregressive with eXogenous Inputs
Attention	Attention Mechanism	OCV	Open Circuit Voltage
DaNN	Domain-Adversarial Neural Network	PCA	Principal Component Analysis
DFNN	Deep Feedforward Neural Network	PINN	Physics-Informed Neural Network
DGMDN	Deep Gaussian Mixture Density Network	Rint-DM	Rint Difference Model
ECS	Equivalent Circuit Simulation	RLS	Recursive Least Squares
FEA	Finite Element Analysis	RVM	Relevance Vector Machine
FFRLS	Forgetting Factor Recursive Least Square	SEI	Solid Electrolyte Interphase
GPR	Gaussian Process Regression	SMO	Sliding Mode Observer
GRU	Gated Recurrent Unit	SPM	Single Particle Model
HMA	Heterogeneous Multi-Physics Aging	SPMT	Single Particle Thermodynamic Model
ICA	Incremental Capacity Analysis	UKF	Unscented Kalman Filter
LightGBM	Light Gradient Boosting Machine	WLS-SVM	Weighted Least Squares Support Vector Machine
LS-SVM	Least Squares Support Vector Machine	WQR	Weighted Quantile Regression

2. Definition of Each State of Lithium-Ion Batteries

The various states of LIBs exhibit complex intrinsic coupling relationships, which dynamically change with battery usage, charge-discharge cycles, and operating environment. Depending on specific application scenarios and system requirements, the same state can be defined and described in multiple ways. Table 3 summarizes the primary definition methods and applicable scenarios for SOC, SOH, SOP, SOE, and RUL.

Table 3. Common states and definitions of lithium-ion batteries.

State Type	Definition Method	Definition Formula	Formula Description	References
SOC	Capacity ratio method	$SOC = \frac{Q_{cur}}{Q_{act}} \times 100\%$	Q_{cur}: Current remaining capacity; Q_{act}: Current actual maximum capacity	Chen et al. [46]; Takyi-Aninakwa et al. [47]; Fan et al. [48]
	Open circuit voltage method	$SOC = f(OCV)$	f: SOC-OCV mapping relationship	Li et al. [49]; Chen et al. [50]; Barcellona et al. [51]
SOH	Capacity fade method	$SOH = \frac{Q_{act}}{Q_{init}} \times 100\%$	Q_{act}: Current available capacity; Q_{init}: Initial capacity of a new battery	Vignesh et al. [52]; Dini et al. [53]; Gao et al. [54]
	Internal resistance method	$SOH_R = \frac{R_{end} - R_t}{R_{end} - R_{init}} \times 100\%$	R_{init}: Initial internal resistance; R_{end}: Internal resistance at the end of life; R_t: Internal resistance at sampling time t	Demirci et al. [55]; Xie et al. [56]; Su et al. [57]
SOP	Power output ratio method	$SOP = \frac{P_{cur}}{P_{\max}} \times 100\%$	P_{cur}: Current power; $P_{\max}$: Maximum power	Shrivastava et al. [58]; Raoofi et al. [59]; Dai et al. [60]

Table 3. *Cont.*

State Type	Definition Method	Definition Formula	Formula Description	References
	Maximum power point method	$SOP = \frac{(V_{OCV} - V_{\min})^2}{R_{in}}$	V_{OCV}: Open circuit voltage; $V_{\min}$: Minimum allowable voltage; R_{in}: Battery internal resistance	Guo et al. [61]; Rojas et al. [62]; Naseri et al. [63]
SOE	Energy ratio method	$SOE = \frac{E_{remain}}{E_{total}} \times 100\%$	E_{remain}: Current remaining energy; E_{total}: Total energy of the battery	Mukherjee et al. [64]; Zhang et al. [65]; Zhang et al. [66]
RUL	Cycle life method	$RUL = \frac{N_{total} - N_{used}}{N_{total}} \times 100\%$	N_{total}: Total design life; N_{used}: Cycles used	Ren et al. [67]; Shan et al. [68]; Uzair et al. [69]

As summarized in Table 3, the primary definition methods and formulas for five common states in LIBs are presented. SOC represents the ratio of the current battery charge to its total capacity, typically expressed as a percentage from 0% to 100% [70]. SOC mainly controls the battery's charge and discharge processes, preventing overcharging and over-discharging, thereby ensuring battery safety and longevity. SOH indicates the battery's current health status, representing the available capacity and power output ratio compared to a new battery's values [71]. Estimating SOH helps determine whether the battery needs maintenance or replacement, extending the overall system lifespan and reducing maintenance costs. SOP represents the maximum power the battery can output or absorb in its current state, reflecting its instantaneous charging and discharging capabilities [72]. SOP is useful for managing power output, optimizing battery performance, and preventing overload. SOE describes the battery's current remaining energy, directly indicating the energy available for output. Monitoring SOE can prevent excessive discharge and ensure reasonable allocation and utilization of energy [73]. RUL is typically estimated regarding the remaining charge-discharge cycles or service time, reflecting the battery's degradation trend and its future usable life [74]. Monitoring RUL helps determine when a battery should be removed from active use, potentially repurposed as a backup power source, or entered into a recycling process.

3. Summary of State Estimation Methods Based on Physical Model

Model-based LIB state estimation algorithms rely on the battery's ECM, EM, thermal, and aging models. These algorithms simulate the battery's internal physicochemical processes by constructing system description equations. They then use a series of state estimation algorithms or numerical computation methods, such as KF, adaptive observers, and FEA, to achieve the final state estimation. Figure 1 illustrates the basic steps of this process.

As shown in Figure 1, there is a wide variety of physical models for LIBs; however, regardless of the model type, certain data types are essential, including current, voltage, temperature, internal resistance, and capacity degradation rate. For example, ECM and EM models require current, voltage, and temperature data; aging models also require cycle data, and thermal models need data on battery temperature, current, and ambient temperature. The same physical model can also be paired with different state estimation algorithms. For instance, ECM, EM, and thermo-electric coupling models can be combined with KF for state estimation. In contrast, both ECM and aging models can be paired with RLS for parameter identification. This high consistency in data types provides a solid foundation for multi-model state estimation fusion algorithms, enabling multi-state joint estimation. Table 4 categorizes recent LIB state estimation methods based on different models.

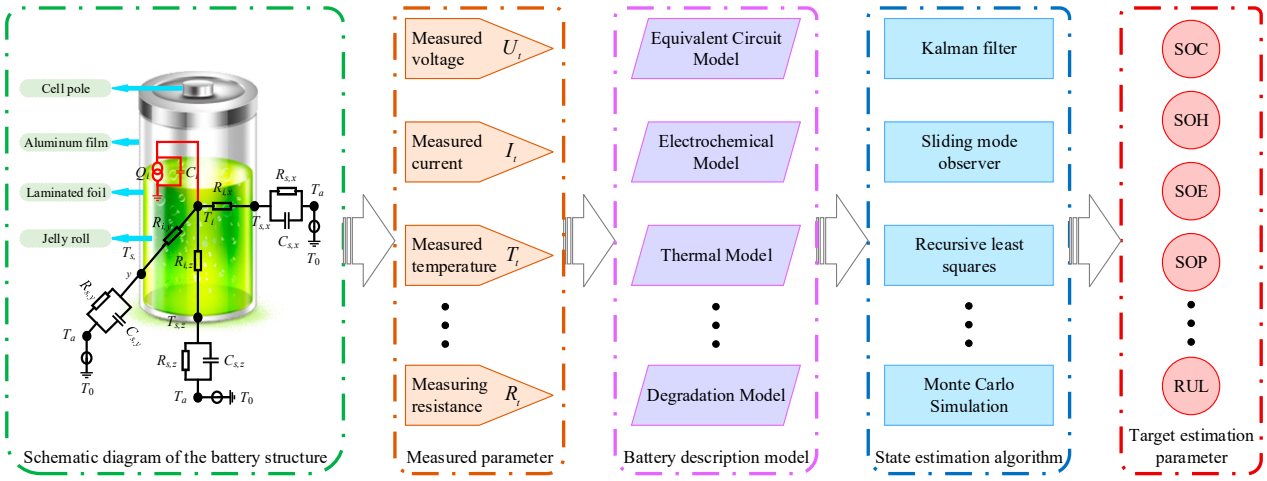

Figure 1. Flowchart of model-based state estimation.

Table 4. Model-based state estimation methods for lithium-ion batteries.

Model Type	Required Data	Primary Applications	Applicable Algorithms	Relevant References
Equivalent circuit model	Current; Voltage; Temperature	SOC, SOH, SOP	EKF; Ampere-hour integration; RLS	Ramezani-al et al. (2023) [75] Rodríguez-Iturriaga et al. (2023) [76] Li et al. (2023) [77] An et al. (2023) [78] Li et al. (2023) [79]
Electrochemical model	Current; Voltage; Temperature	SOC, SOH, SOE, RUL	EKF; PF; FEA; Differential equation	Wang et al. (2023) [80] Feng et al. (2024) [81] Hashemzadeh et al. (2024) [82] Yu et al. (2024) [83] Yu et al. (2023) [84]
Thermo-electric coupling model	Current; Voltage; Battery Temperature; Ambient Temperature	SOC, SOE, RUL	EKF; PF; FEA	Chen et al. (2024) [85] Zeng et al. (2024) [86] Xu et al. (2023) [87] Liu et al. (2023) [88] Gayathri et al. (2024) [89]
Aging model	Current; Voltage; Temperature; Cycle Count	SOH, RUL	RLS; Monte Carlo simulation; Time series analysis	Li et al. (2024) [90] Fang et al. (2023) [91] Zhang et al. (2023) [92] Hofmann et al. (2024) [93] Wang et al. (2023) [94]

3.1. Methods Based on Equivalent Circuit Models

As shown in Table 4, LIB state estimation involves various models, each with its own characteristics, suitable for different application requirements and estimation accuracy needs. Among these, the ECM uses resistors, capacitors, and other equivalent components to simulate the electrochemical behavior of the battery. It is currently one of the most widely used simplified modeling methods. ECM is popular due to its relatively low computational complexity, strong parameter identification and adaptability, clear physical interpretation, and suitability for the joint estimation of multiple battery states. Figure 2 presents several typical ECM structures to help readers understand their working principles and differences more intuitively.

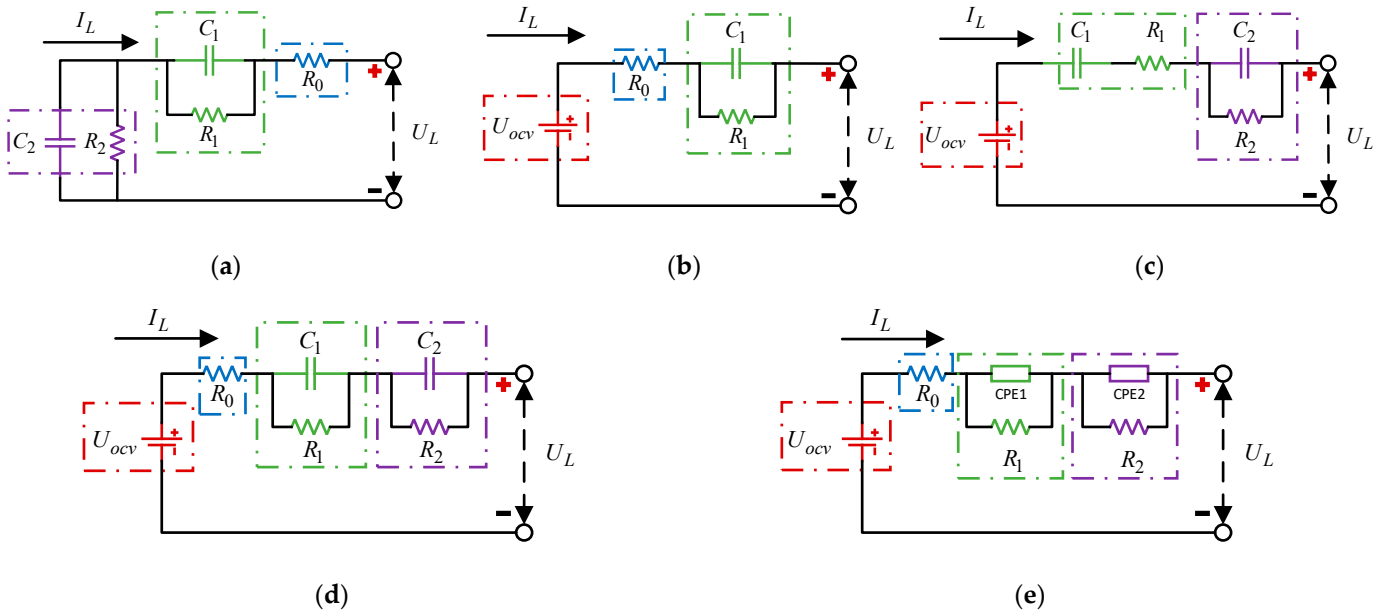

Figure 2. Common types of equivalent circuit models. (**a**) Randles ECM; (**b**) Thevenin ECM; (**c**) PNGV ECM; (**d**) Second-order RC ECM; (**e**) Fractional-order ECM.

Ramezani et al. [75] proposed a new method that combines direct measurement techniques with EKF state estimation. In the linear part of the OCV-SOC curve, the OCV is directly estimated using RLS to calculate SOC. In the nonlinear region, an EKF-based estimation is performed by combining a second-order RC model, which reduces the computational burden of EKF while maintaining high estimation accuracy under different conditions. Rodríguez-Iturriaga et al. [76] innovatively linked physical parameters directly to the ECM, using ZARC components and CPE to model the diffusion and charge transfer processes in LIBs. They incorporated electrochemical measurement data to improve the model accuracy, ultimately providing more accurate battery state estimation while ensuring lower computational complexity. Li et al. [77] proposed a multi-timescale SOC and SOP joint estimation strategy based on a second-order RC model and H∞ filter, utilizing FFRLS for online model parameter identification. SOP estimation is based on the battery terminal voltage, current SOC, and design constraints, and it uses a combination of voltage, current, and SOC constraints to obtain continuous peak power. An et al. [78] used a thermo-electric coupled ECM to simulate the voltage and temperature responses of the battery, combining EKF for SOC estimation to support prediction-based SOE estimation. The model integrates electrical and thermal effects, with the electrical part using the Thevenin model, accounting for Ohmic and polarization voltage drop. In contrast, the thermal effects include heat generation and dissipation, enabling temperature prediction. Li et al. [79] combined ECM with UKF for SOC estimation and used GPR for SOH estimation while predicting RUL with LS-SVM. This approach improves the adaptability of ECM parameters to SOH, allowing the impedance and capacitance parameters in the model to adjust dynamically according to the aging state of the battery, ensuring the stability and reliability of SOC estimation in complex aging scenarios.

3.2. Methods Based on Electrochemical Models

The EM describes the complex reaction mechanisms, transport processes, and charge balance within electrochemical systems like batteries by modeling the movement and reactions of ions, electrons, and molecules inside the battery. State estimation methods based on EM offer significant advantages, including high precision, a deep understanding of battery behavior, strong scalability, adaptability to complex operating conditions, and support for battery life prediction and safety management. These capabilities make EM

highly valuable in BMS, especially in enhancing battery performance, safety, and life prediction. Figure 3 shows two common types of EMs: the SPM and the P2D model.

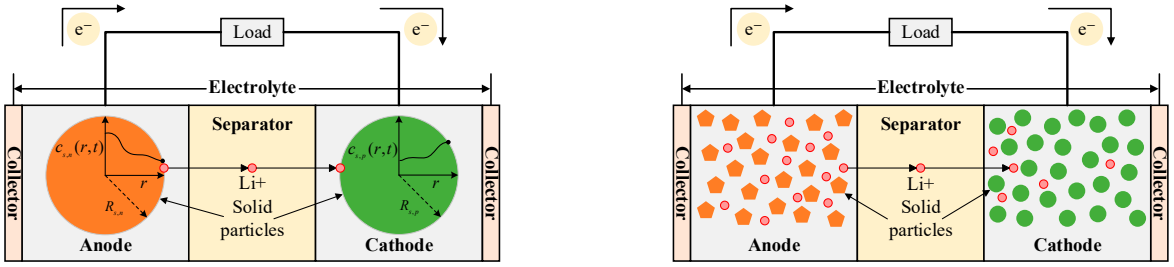

(**a**) (**b**)

Figure 3. Schematic diagrams of the SPM and P2D model. (**a**) Single particle model; (**b**) Pseudo-2D model.

Wang et al. [80] proposed a simplified version of the SPM with low complexity, which maintains the ability to describe the internal reaction characteristics of the battery while mitigating the high computational burden associated with the traditional P2D model. This approach incorporates a PF for voltage feedback correction, enhancing the accuracy and stability of SOC estimation. Feng et al. [81] introduced a method based on SPM, utilizing a cascade SMO for joint estimation of SOC and SOH in LIBs. The hierarchical design of multiple SMOs enables step-by-step estimation of lithium-ion concentrations at different nodes within the battery, effectively reducing estimation errors and achieving layer-wise convergence. Hashemzadeh et al. [82] presented a nonlinear enhanced version of SPM, which innovatively incorporates concentration-dependent electrolyte parameters to more accurately capture the dynamic behavior of the battery. This method uses an orthogonal configuration approach to approximate the distribution of lithium-ion concentration. It employs a three-parameter second-order polynomial approximation to significantly simplify the computational complexity, thereby improving the real-time performance and reliability of the model. Yu et al. [83], building on the traditional P2D model, introduced a simplification strategy that reduces the model's computational complexity, particularly by eliminating detailed calculations of electron and ion concentration variations in the full-order physical model. They also proposed an optimization strategy for parameter merging, combining multiple related parameters into a set of independent and simplified parameters. They optimized the partial differential equations and modeled the finite difference method for the numerical solution to facilitate the rapid and accurate solution of the model's parameters and outputs. Yu et al. [84] proposed a multi-scale modeling approach based on a simplified SPM to develop a simple yet self-consistent multi-particle simplified EM to study the effects of different particle sizes on SEI film growth. Moreover, they constructed a fast, simplified SEI film growth model based on Kinetic Monte Carlo simulations, which can model the morphological evolution of the SEI film over extended time scales while maintaining low computational cost.

3.3. Methods Based on Thermoelectric Coupling Models

Batteries generate heat during the charging and discharging cycles, affecting their electrochemical performance. The thermo-electrochemical coupling model integrates the battery's electrochemical reactions and thermal effects, offering a comprehensive representation of the complex internal processes. This model provides an improved ability to account for temperature fluctuations and more accurately reflects the battery's operational state. Chen et al. [85] developed a thermo-electrochemical coupling model for the 21,700-type cylindrical LIB. They conducted experiments under various temperature conditions and extracted key parameters, revealing variations over a wide temperature range (−20 °C to 40 °C). Unlike traditional uniform heat source models, this approach can simulate non-

uniform temperature distributions while maintaining lower computational complexity than both ECM and conventional thermo-electrochemical models. Zeng et al. [86] introduced an asynchronous fractional-order thermo-electrochemical model based on frequency characteristic separation. Using EIS, the model separates parameters across different time scales in the frequency domain, ensuring that each parameter is updated at a rate corresponding to its physical behavior. Multiple asynchronous filtering algorithms were employed for real-time parameter identification, improving the coupling of dynamic parameters and thereby enhancing model accuracy. Xu et al. [87] proposed a multi-layer thermo-electrochemical coupling model for LIB systems. The model combines the Thevenin equivalent to describe electrical characteristics and integrates it with a thermal transfer model to simulate battery behavior under various ambient temperatures, cooling conditions, and current inputs. To enhance the model's accuracy and adaptability, key parameters, such as resistance and capacitance, are dynamically adjusted in real time based on experimental temperature and battery state mappings, enabling the model to effectively capture the variations in battery behavior under diverse conditions. Liu et al. [88] addressed the challenge of non-linear coupling between thermal and electrical parameters in traditional models, which is difficult to solve in real time. By decoupling the thermal and electrical parameters, they used offline experiments under constant current, employing Nernst and Arrhenius equations to derive open-circuit voltage, internal resistance, and temperature data. State calculations were standardized using Coulombic efficiency coefficients to ensure accuracy. Gayathri et al. [89] proposed a hybrid multi-model approach for thermo-electrochemical modeling, integrating four local models. The model uses a genetic algorithm to optimize the charging curves, improving prediction accuracy. Furthermore, it supports dynamic charging current adjustment for various applications, offering multiple charging strategies to meet different user needs.

3.4. Methods Based on Aging Models

Battery state estimation based on aging models focuses on describing and predicting the aging process of LIBs. Tracking the performance degradation of the battery during use provides accurate estimates of the SOH of LIBs, offering effective support for BMS. Li et al. [90] proposed an online SOH estimation algorithm based on a linear parameter-varying model. The model combines a local linear dynamic model with a global nonlinear degradation model, allowing it to capture both the rapid dynamic changes and gradual degradation of LIBs throughout their entire lifecycle. This design effectively decouples the coupling effect between SOC and SOH, enabling the model to handle SOC separately related to instantaneous dynamics and SOH related to long-term aging. Fang et al. [91] developed an improved SPM by coupling three different SEI film growth mechanisms with the SPM. The effects of aging are incorporated into the parameter estimation method to accurately predict LIB performance throughout its lifecycle. Zhang et al. [92] extracted key features such as SEI film resistance, SEI characteristic time constant, and Ohmic resistance and employed an NN-based aging model. The extracted EIS features were inputs to estimate the battery's SOH. Additionally, time-domain methods like differential voltage analysis were applied to explore the aging mechanisms, helping to identify the most significant features that reflect the battery's aging process. Hofmann et al. [93] proposed the ΔQ method, a novel SOH decay estimation model for LIBs based on battery relaxation voltage points and cumulative charge. This method reconstructs the OCV curve. It estimates SOH by optimizing the charge difference between various relaxation voltage points, thus reducing reliance on complex and costly long-term data collection while improving applicability to real-world data. Wang et al. [94] proposed a SOH estimation method based on ICA combined with charge/discharge rates. First, they applied a finite-time differentiator to smooth the raw ICA curve from high-frequency sampled data. Then, several experiments were designed to account for different initial SOC and charge/discharge rates, analyzing the impact of these variables on health characteristics and ICA curves.

4. Summary of State Estimation Methods Based on Data-Driven Models

In recent years, data-driven models for LIB state estimation have become a significant research direction in BMS. Common data-driven approaches include machine learning, deep learning, and statistical analysis. These models primarily rely on historical data and data mining techniques to estimate battery states. The data typically comes from experimental tests or real-world operating conditions, including sensor information such as current, voltage, and temperature. In applying data-driven models for battery state estimation, the data quality directly impacts the model's accuracy, making data preprocessing and feature engineering crucial. Figure 4 illustrates the basic workflow of LIB state estimation based on data-driven models.

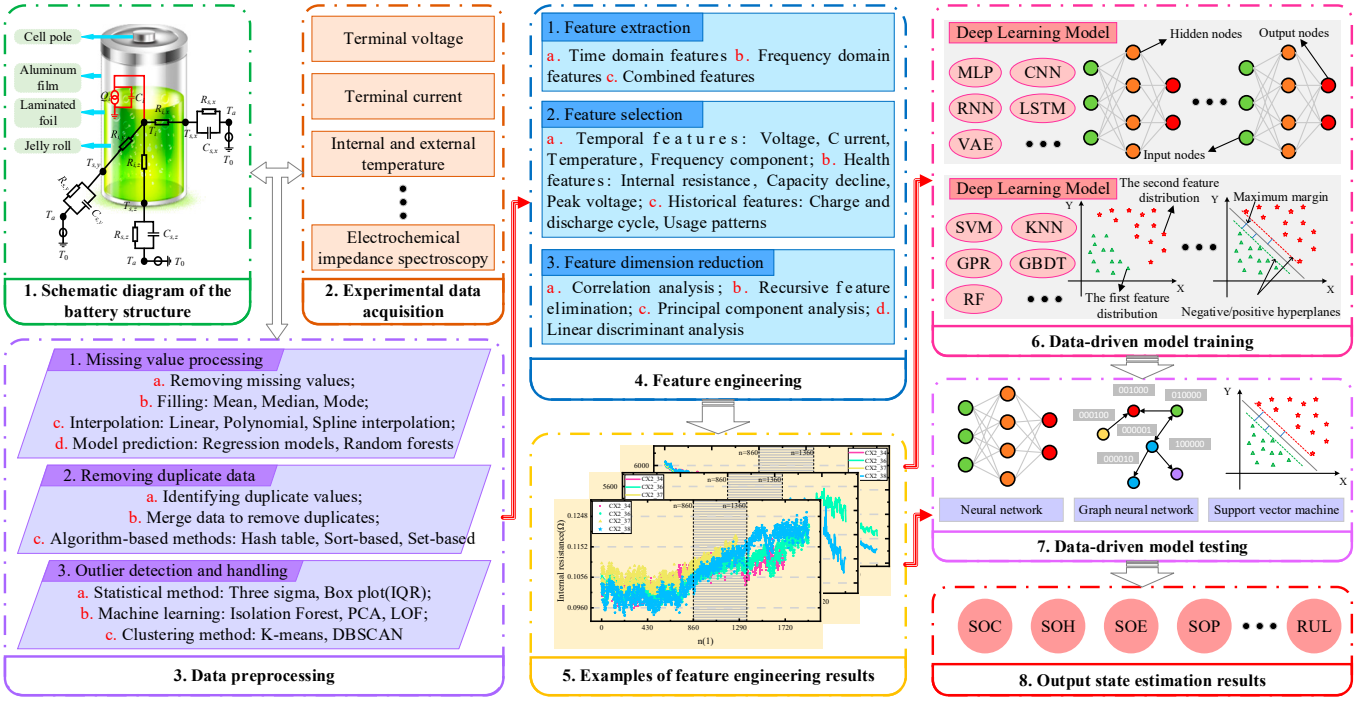

Figure 4. Flowchart of state estimation based on data-driven models.

As shown in Figure 4, the core of data-driven LIB state estimation lies in the dataset, which does not rely on complex electrochemical equations or ECMs. The model provides rich battery feature information by collecting large amounts of historical data, such as voltage, current, and temperature. This highlights the critical importance of data preprocessing. Before the data is input into the model, it must undergo cleaning, outlier removal, and missing data imputation to ensure the quality of the input data. Feature extraction is a key step in LIB state estimation. Direct measurements, such as voltage, temperature, and current variations over time, represent time-domain features that reflect the real-time state of the battery during the charge and discharge processes. Additionally, parameters such as voltage decay rate, capacity degradation, and charge/discharge slope can reflect the long-term aging characteristics of the battery. By performing frequency-domain analysis, such as Fourier or wavelet transforms, on these time-domain signals, the internal electrochemical processes of the battery can be revealed. For example, high-frequency components may be associated with the battery's internal resistance, while low-frequency components may be related to battery capacity and SOH. Frequency-domain features are useful for identifying state changes under different operating conditions and are particularly effective in feature extraction in complex, noisy environments. Table 5 presents a series of recent LIB state estimation methods based on data-driven models, categorized into supervised and unsupervised learning approaches. Due to the limited application of reinforcement learning in LIB state estimation, this paper does not discuss this aspect.

Table 5. Lithium-ion battery state estimation method based on data-driven model.

Learning Method	Base Model Name	Algorithm Abbreviation	Target Estimated State	Relevant Literature
Supervised learning	SVM	WLS-SVM	RUL	Xiong et al. (2023) [95]
	ANN	Elman-NN	SOT	Wang et al. (2023) [96]
	LSTM	SA-LSTM	RUL	Wang et al. (2023) [97]
	RF	NN-RF-BO	RUL	Zhang et al. (2023) [98]
	GBDT	LightGBM-WQR	SOH	Qin et al. (2023) [99]
Unsupervised learning	K-Means	KMC-GBP	SOC	Hai et al. (2023) [100]
	GMM	DGMDN	SOH	Fei et al. (2023) [101]
	PCA	PCA-PSO-BPNN	SOH	Wu et al. (2023) [102]
	Autoencoder	CD-Net	RUL	Sudarshan et al. (2024) [103]
	DBSCAN	DFMF	SOH	Zeng et al. (2023) [104]

4.1. Methods Based on Supervised Learning

Supervised learning is a method that utilizes labeled training data to make predictions. Supervised learning is widely used in LIB state estimation to predict various battery state parameters, such as SOC, SOH, and RUL. As shown in Table 4, regression models are one of the most commonly used methods in supervised learning. Xiong et al. [95] applied SVM to predict the changes in battery capacity over its entire lifecycle. A weighted least squares method was introduced to weigh the error variables, enabling the WLS-SVM to prioritize reliable data points and reduce the influence of outliers on the model. Deep learning methods such as CNN and LSTM are also applied for more complex battery dynamics for state estimation, as they can better capture the nonlinear and sequential characteristics of battery behavior. Wang et al. [96] used Elman-NN to predict the temperature changes in LIBs. Elman-NN is an improvement based on artificial neural networks, where a feedback mechanism is added to handle sequential and time-series data. This design laid the foundation for later RNNs like LSTM and GRU. Wang et al. [97] proposed a predictive model using adaptive self-attention LSTM, which integrates a masked multi-head self-attention module with LSTM to capture key features within time-series data. This approach enhances long-term prediction performance while reducing reliance on irrelevant information. Feature extraction and feature selection become particularly important to improve model performance, especially when methods such as SVM, RFR, and GBDT are used. This helps reduce redundancy and improve prediction accuracy. Zhang et al. [98] extracted charging features through dilated convolution networks, enhanced discharge features with DNN, and then fused these features into an RFR model to predict LIB cycle life. Qin et al. [99] proposed using the complete charging voltage curve as an input feature to estimate SOH, which reduces feature redundancy without affecting model estimation accuracy. They employed weighted quantile regression to obtain uncertainty information for the SOH estimate and applied quantile regression in a LightGBM model to provide SOH estimate intervals.

The advantage of supervised learning lies in its high accuracy and robustness, particularly when data is abundant and of high quality. Models trained on large volumes of historical data can effectively estimate battery states.

4.2. Methods Based on Unsupervised Learning

Unsupervised learning is a method that does not require labeled data, and it plays an important role in LIB state estimation, especially in cases where labeled data is scarce or unavailable. Clustering methods in unsupervised learning, such as K-means, density-based spatial clustering of applications with noise, and hierarchical clustering, are widely used for analyzing and classifying LIB degradation patterns. By clustering historical battery data, different degradation modes of the battery can be identified, which helps recognize groups of batteries with similar health states. Hai et al. [100] divided the data into multiple clusters and applied K-Means for local optimization within each cluster, allowing the

genetic algorithm to avoid complex global searches. By defining the fitness function of the K-Means clustering, they dynamically adjusted the crossover and mutation probabilities of the genetic algorithm, enhancing its adaptability to complex data. Fei et al. [101] used a model based on a DGMDN to fuse the extracted features and generate the conditional probability distribution of battery SOH. The model, trained by maximizing the likelihood function, provides point estimates and uncertainty measures for SOH, enabling more reliable battery health assessments. Zeng et al. [104] used density-based spatial clustering of applications with noise to detect sensor faults from raw voltage, charge, and temperature data, combined with a state machine-based fault isolation method, ensuring that SOH estimates rely only on data from properly functioning sensors. Finally, ridge regression was used for SOH estimation across multiple sensor data, improving computational efficiency and reducing the complexity of nonlinear models.

In battery state estimation, the features collected are often high-dimensional, leading to issues with information redundancy. Dimensionality reduction methods in unsupervised learning, such as PCA and autoencoder, can map high-dimensional features to lower-dimensional spaces, making it easier to uncover trends and patterns in the data. Wu et al. [102] extracted six features related to battery aging from NASA's battery aging test data. After performing PCA for dimensionality reduction, the input features were reduced from six to two, significantly simplifying the model's complexity. The features optimized by PCA showed stronger correlations with SOH in grey relational analysis. Sudarshan et al. [103] designed a self-encoding neural network called CD-Net. CD-Net employs an architecture combining sequence autoencoders and perceptrons, where the sequence autoencoder handles noise reduction and time-series feature extraction, and the perceptron captures complex degradation mechanisms. The model predicts the future battery capacity state using historical cycling data and other features (such as battery chemistry and rated capacity).

Unsupervised learning is particularly useful when underlying patterns in data need to be discovered. It helps understand complex battery data structures and reveals critical battery health information. This is especially valuable in applications that lack large amounts of labeled data or aim to uncover unknown patterns.

5. Summary of Algorithms Based on Multi-Physics Models and Data-Driven Model Fusion

Multimodal fusion is an approach that integrates various types of models, aiming to enhance overall system performance and prediction accuracy by combining the strengths of multiple models. In the context of LIB state estimation, multimodal fusion is a highly effective strategy, achieving more precise and robust state estimation by combining physical and data-driven models. Each model in a multimodal fusion approach has its specific domain of application and suitability conditions. For example, physical models are based on physical laws, offering good interpretability and are suitable for describing the internal dynamic characteristics of a system. On the other hand, data-driven models excel at capturing complex nonlinear relationships from historical data. They can still provide high-accuracy estimates even when explicit physical laws are unavailable. This paper divides the multimodal fusion strategy into three categories: fusion of multiple physical models, fusion of multiple data-driven models, and hybrid fusion combining physical and data-driven models.

5.1. Methods Based on Multi-Physics Model Fusion

During the operation of LIBs, complex internal interactions occur, including electrochemical reactions, thermal effects, mechanical stress changes in materials, and fluctuations in electrical performance. By integrating the mathematical descriptions of these physical processes, such as EM, ECM, and thermal models, multi-physics model fusion enables a more comprehensive understanding and prediction of the dynamic behavior of LIBs. This integration enhances the accuracy of key state parameter estimation. Table 6 presents various multi-physics model fusion algorithms proposed in recent years.

Table 6. Multi-physics model fusion algorithm.

Base Model Name	Relied Physical-Chemical Mechanisms	Base Algorithms	Target Estimated States	Related References
Improved Electro-thermal Aging Multi-Physics Coupling Model	Second-order RC model, simplified thermal path model, slow capacity degradation phenomenon	AMTDIE, FFRLS, EKF	SOC, SOT, SOH	Shi et al. (2024) [105]
Electrochemical-Thermal-Aging Coupling Model	SEI layer formation and growth, lithium deposition, manganese dissolution and migration	Arrhenius empirical formula, Butler–Volmer equation, Bernardi equation	SOT, SOH	Xi et al. (2024) [106]
HMA Model	Active material loss, diffusion-induced stress, SEI layer formation and growth	Least squares fitting method, boundary parameter determination method	SOH, RUL	Wang et al. (2023) [107]
Electrochemical-Thermal-Aging Coupling Model	Electrochemical reaction kinetics, SEI layer formation, lithium metal deposition, thermodynamic model	MPC, UKF	SOC, SOH, RUL	Zhou et al. (2024) [108]
Thevenin Model—Second-Order RC Model	Battery electrochemical characteristics analysis based on Shepherd and Nernst models	FFRLS, UKF, Bayesian fusion with probability weighting, RLS	SOC	Li et al. (2023) [109]

As shown in Table 6, Shi et al. [105] proposed a multi-physics coupling model to describe the complex dynamic behavior of LIBs. This model integrates the battery's electrical, thermal, and aging characteristics. The second-order RC model simulates the battery's charge transfer, diffusion, and electrochemical reactions. Based on the first law of thermodynamics, a lumped parameter model is used to describe the thermal conduction behavior between the battery's interior and surface using thermal resistance and capacitance parameters. The aging model describes the capacity degradation process over time, and different time-scale control strategies are employed to estimate the battery's available capacity. Xi et al. [106] designed a multi-scale, multi-physics coupling model to describe the complex dynamics of the battery under varying temperatures and operating conditions. In the electrochemical model, based on the P2D framework, conservation equations, and the Butler–Volmer equation are used to describe the diffusion, concentration changes, and charge conservation of lithium ions in both the electrolyte and solid phases. In the thermal model, the Bernardi equation is used to describe the heat conservation and generation characteristics of the battery under different operating conditions, allowing for the prediction of the average temperature of the battery. In the aging model, the SEI layer's growth, regeneration, and lithium plating formation are considered. The model uses the Arrhenius empirical formula to describe the relationship between temperature and aging reactions, capturing the interactions between thermal and electrochemical behaviors, especially the acceleration of aging reactions at higher temperatures and their impact on overall battery performance. Wang et al. [107] proposed an HMA-based fault diagnosis method for LIBs. This model combines multiple physical-chemical mechanisms, such as the formation and thickening of the SEI film, stress-induced crack propagation due to diffusion, and structural changes in the anode and cathode materials, to accurately simulate the complex aging process inside the LIB. Key parameters, such as OCV and internal impedance, are identified through the RLS fitting method to calibrate the model, allowing it to accurately reflect the battery's state at different aging stages. Furthermore, the method simulates multiple sets of combinations of high-sensitivity parameters. It performs three-dimensional spatial fitting to build parameter boundaries for online SOH diagnosis, providing fault warnings for capacity degradation at critical points to ensure the performance and safety of the battery in practical applications. Zhou et al. [108] designed a multi-physics coupling battery model, combining electrochemical, thermal, and aging sub-models to simulate the LIB's internal state and aging mechanisms. By constructing an extended SPM, the model can accurately capture lithium-ion diffusion, SEI layer growth, and heat generation and conduction inside the battery. The study uses an MPC algorithm to predict the battery's behavior over time

and determine the optimal charging current under constrained conditions to dynamically control voltage, temperature, and aging processes. In addition, the model combines the UKF to estimate unmeasurable variables inside the battery in real time, enabling SOH monitoring and optimization control. Li et al. [109] combined the Thevenin model and the second-order RC model to more comprehensively capture the dynamic characteristics of the battery. First, the Thevenin and second-order RC models describe the battery's dynamic behavior under different operating conditions, with the model parameters determined through RLS. To improve the accuracy of SOC estimation, UKF is used, with iterative corrections to the SOC estimates. In multi-model fusion, Bayesian theory is applied to assign optimal weights to the two models and merge the SOC estimates from different models to form a more precise final estimate. Moreover, to enhance the algorithm's adaptability under complex operating conditions, the study introduces a residual innovation sequence that allows the window width to be adaptively adjusted, optimizing the UKF performance.

Multi-physics model-based LIB state estimation has become a key area of research in BMS and control fields. By integrating ECM, EM, thermal models, and mechanical models, it is possible to comprehensively describe the complex behaviors of LIBs, significantly improving the accuracy of key parameter estimates like SOC and SOH. However, several challenges remain despite the strong potential of multi-physics models for battery state estimation. These models often involve multiple parameters (e.g., resistance, capacitance, diffusion coefficients), and the complexity of electrochemical and thermal models demands substantial computational resources, creating a high technical barrier for real-time applications. Additionally, electrochemical, thermal, and mechanical stress coupling under high-power charge and discharge conditions can trigger dramatic changes in LIB characteristics. Therefore, rationally designing the coupling relationships between different physical models is essential for better capturing these interactions and improving the precision and reliability of state estimation.

5.2. Methods Based on Multi-Data-Driven Model Fusion

In data-driven modeling, the fusion of multiple machine learning or statistical models can significantly enhance state estimation accuracy and improve the model's generalization ability. For instance, combining models like RF, SVM, and NN through ensemble learning techniques can improve the ability to capture complex data patterns while increasing resilience to data noise and anomalies. Recently, multi-data-driven model fusion in LIB state estimation has become more widespread. Table 7 outlines the latest developments in various related algorithms.

Table 7 shows that Sun et al. [110] proposed a deep learning-based CNN-BiLSTM-Attention model. This model uses CNN to extract spatial relationships from input features, captures bidirectional dependencies in time series through BiLSTM, and incorporates the Attention mechanism to focus on key information, thereby improving estimation accuracy. Additionally, the model introduces a three-parameter Weibull distribution as an extra feature to describe the effect of battery inconsistency on SOC. This method achieves high-precision SOC estimation by fusing multi-dimensional time-series signals, showing particularly strong performance in the low SOC region, where battery behavior is more volatile. Zhang et al. [111] proposed a multi-model fusion approach to enhance SOH estimation performance using four machine learning algorithms: GPR, BRR, RFR, and DNN. These algorithms are independently trained to capture different data features (such as voltage variations, charging time, current curves, etc.), each demonstrating its strengths in complex dynamic operational environments. They introduced a KF to combine the estimation results from the four machine learning algorithms with histogram-based predictions, systematically incorporating each model's uncertainty quantification output to achieve optimal model fusion. Xiong et al. [112] used GPR to reconstruct incomplete charging data, supplementing health features when random charging constraints limit data availability. Then, the LSTM model is employed for SOH estimation based on the GPR-reconstructed data. LSTM avoids complex feature extraction and effectively utilizes the random charg-

ing data. This method enables accurate SOH prediction even when the charging data is incomplete and random. Xia et al. [113] combined the time-series prediction capabilities of the NARX model with the efficient feature extraction of the DS-Attention mechanism to improve SOH and SOC prediction accuracy for LIBs. The NARX model models complex nonlinear relationships by inputting historical states and external control variables, while the DS-Attention mechanism optimizes the attention mechanism by introducing segmentation and adaptive functions. The segmentation function separates external inputs from state outputs to avoid mutual interference, and the adaptive function integrates query features from the entire sequence to generate a more reasonable attention benchmark. Wang et al. [114] first used the multi-core incremental RVM to build a data-driven model to capture the complex nonlinear relationship between voltage, current, and SOC. They then introduced the SARIMA algorithm as the state equation, modeling time series to smooth SOC predictions and overcoming the limitations of traditional coulomb counting methods. Next, they applied AEKF to filter the outputs of the seasonal autoregressive integrated moving average model, further improving the stability and accuracy of the estimation. Finally, the whale optimization algorithm optimized model parameters, achieving efficient real-time SOC prediction.

Table 7. Multiple data-driven model fusion algorithm.

Fusion Type	Base Models	Fusion Theory Basis	Target State Estimation	Relevant Literature
Spatiotemporal feature fusion neural network	CNN, Bi-LSTM, Attention Mechanism	Spatiotemporal feature decomposition and fusion, Enhanced nonlinear mapping, Selective focusing via attention mechanism	SOC	Sun et al. (2024) [110]
Data-driven multi-model fusion Kalman filtering	GPR, BRR, RFR, DNN	Quantification of uncertainty from multi-source heterogeneous models, Dynamic weighted fusion with Kalman filtering	SOH	Zhang et al. (2024) [111]
Gaussian process reconstruction-memory fusion under random charging	GPR, LSTM	Synergy between data reconstruction and sequence modeling, Enhanced by uncertainty quantification	SOH	Xiong et al. (2023) [112]
NARX-DS adaptive separation attention network	NARX model, DS Attention Mechanism	Feature separation of exogenous inputs and state outputs, Adaptive weight optimization, Closed-loop NARX to enhance prediction accuracy	SOC, SOH	Xia et al. (2024) [113]
Multi-kernel incremental regression with seasonal adaptive filtering	Multi-kernel Incremental RVM, Seasonal ARIMA, AEKF	Adaptive integration of multiple kernel functions, Combination of time-series prediction and dynamic filtering, Optimal parameter adaptive tuning	SOC	Wang et al. (2023) [114]

Each model may be based on different datasets, feature selections, or algorithms. By fusing multiple data-driven models, the strengths of data and models from various sources can be integrated, reducing the limitations of individual models and improving prediction accuracy and model robustness. However, this approach also presents several inherent challenges. First, the fusion of multiple data-driven models heavily depends on large amounts of high-quality data. If the volume or quality of the data is insufficient, it will directly impact the model's performance. Additionally, the joint training of multiple models and large-scale data processing result in high computational costs. Moreover, the singularity of data sources may lead to models failing to fully uncover the hidden information within the dataset, increasing the risk of overfitting. To address these challenges, combining physical models of LIBs with data-driven models offers a promising direction. This fusion approach leverages richer data and applies physical prior knowledge to guide the training of data-

driven models, effectively reducing the risk of overfitting while significantly enhancing the model's generalization ability and prediction accuracy.

5.3. Methods Based on the Fusion of Multi-Physics and Data-Driven Models

Integrating physical models with data-driven models is one of the most popular fusion methods in current research. This approach effectively combines the strengths of both multi-physical and data-driven models to achieve high-precision state estimation for LIBs. Multi-physical models are based on various physical mechanisms, such as electrochemical, thermoelectric, and mechanical models, which simulate the intrinsic characteristics of batteries. These models provide systematic prior knowledge and physical constraints. On the other hand, data-driven models leverage machine learning and deep learning techniques to train on historical data, learning the behavior of LIBs under various operating conditions. This allows data-driven models to compensate for the limitations of physical models in complex scenarios. For example, data-driven models can effectively correct systematic errors in physical models or dynamically update the parameters of physical models based on new data, thus enhancing the accuracy and robustness of state estimation. Table 8 presents a variety of algorithms for the fusion of multi-physical and data-driven models proposed in recent years.

Table 8. Multi-physics model-data-driven model fusion algorithm.

Fusion Theory Basis	Physical Model	Data-Driven Model	Target Estimated State	Related Literature
SPMT-derived features fed into BiLSTM	SPMT	BiLSTM	SOT	Pang et al. (2023) [115]
Bayesian-based multi-network fusion	Second-order RC model	RVM	SOC	Mao et al. (2023) [116]
ECS structure-based fusion LSTM model	ECS layer	LSTM	RUL, SOH	Nguyen et al. (2023) [117]
Physics-based direct fusion in PINN	Battery thermal and chemical dynamic physical models	PINN	SOT	Kim et al. (2023) [118]
Multi-physics data for neural network training	Thermal models, P2D models, and degradation models	CNN, YOLO	SOT	Goswami et al. (2024) [119]
ECM-based modeling with data-driven deep learning	Second-order RC model	ILSTM	SOC	Wang et al. (2024) [120]
Novel mean-difference fusion for AR and ECM	Rint-DM	AR-MM	SOC	Liu et al. (2023) [121]
Multi-state estimation with GRU and Ampere-hour integration	Ampere-hour integration	GRU	SOC, SOH	Zhang et al. (2024) [122]
EIS-based physical info for DaNN training	EIS	DaNN, GPR	SOH	Wu et al. (2024) [123]
ECM-based DFNN fusion architecture	Second-order RC model	DFNN	SOC	Murawwat et al. (2023) [124]
Physics degradation model-constrained BNN	Failure prediction model	BNN	RUL	Najera-Flores et al. (2023) [125]
Physics-based degradation-constrained neural network training	Empirical degradation model	DFNN	SOH	Wang et al. (2024) [126]
Multi-physics, multi-scale fault prediction via local conservation principles	Energy conservation and momentum conservation principles	Local curvature information and model-independent of training data	RUL	Kouhestani et al. (2023) [127]

As shown in Table 8, hybrid methods have been widely applied in predicting the state of LIBs. These methods achieve higher estimation accuracy and reliability by combining the physical interpretability of physical models or EM with the strong ability of data-driven models to handle complex nonlinear relationships. Below, the relevant research is systematically classified and analyzed based on four common hybrid strategies.

(a) Physical models generate initial predictions, and data-driven models correct the errors.

One common hybrid approach involves first generating an initial prediction of the LIB state using a physical model, followed by error correction using a data-driven model. This strategy serially connects the two models, taking full advantage of the physical interpretability provided by the physical model while compensating for prediction errors with the data-driven model to improve overall prediction accuracy. For example, Mao et al. [116] combined the second-order RC model with global FFRLS and UKF algorithms for parameter identification and SOC estimation under normal operating conditions. Additionally, the RVM was introduced to address the shortcomings of the ECM under low-temperature conditions. To effectively combine the strengths of the two models, they proposed a Bayesian-based probabilistic fusion algorithm to calculate the final SOC estimate. Wang et al. [120] applied an improved AEKF and dynamic FFRLS method to achieve SOC estimation under various temperatures and operating conditions. Furthermore, the improved LSTM network with a sliding window multi-to-one structure processed time-series data to compensate for the estimation errors generated by AEKF when higher-order terms were neglected. Murawwat et al. [124] used the second-order RC model to describe the dynamic characteristics of the battery and combined it with UKF for SOC estimation. A DFNN was employed to correct the residuals from the UKF output dynamically, optimizing the SOC estimation accuracy in real time.

(b) Physical model for feature extraction and data-driven models for state estimation

Another hybrid strategy is to use physical models for feature extraction to capture the intrinsic physical characteristics of the system. In contrast, data-driven models are used for state estimation of the LIB. This strategy fully utilizes the detailed modeling of battery characteristics by physical models, providing more accurate input for data-driven models, thus improving the precision of state estimation. Pang et al. [115] adopted PINN as an overall framework, combining the SPMT thermal model with BiLSTM to estimate the heat generation rate of the LIB. The SPMT model provides thermal physical characteristics of the battery, such as electrode surface concentration, which are used as inputs for BiLSTM. This effectively integrates physical knowledge into the data-driven model, enhancing the accuracy of heat generation rate estimation. Nguyen et al. [117] proposed combining an equivalent circuit simulation deep neural network architecture with transfer learning to predict the LIB's RUL. In the first stage of the network, the ECS layer simulates the battery's equivalent circuit, mapping input features into a space related to the battery's ohmic resistance and capturing the battery's SOH. Subsequently, the network adopts an LSTM-based layered architecture, including fully connected regression and dropout layers, to capture the complex relationships between features and SOH and ultimately predict RUL. Goswami et al. [119] combined the P2D and thermal models, using FEA methods to simulate the thermal–electrical coupled behavior of the LIB. They generated thermal images of the battery surface through simulation. They classified them into different temperature thresholds (safe, critical, and uncontrollable) to provide data for training subsequent deep learning models. Then, CNN was used to perform three-class classification on the simulated thermal images and combined with EfficientNetB7 and YOLOv5 models for thermal runaway state identification and hotspot location, enabling more accurate state monitoring. Wu et al. [123] used hierarchical decision graphs and sequential forward search strategies for feature selection from full-frequency EIS data, identifying representative impedance features. They then introduced DaNN and CNN to extract multidimensional information from the EIS features. The model architecture was constructed using pooling and fully connected layers, performing feature fusion and initially predicting SOH. Furthermore, GPR was employed for secondary prediction to improve the accuracy and stability of SOH estimation.

(c) Physical models are used for constraint and interpretation, and data-driven models are used for state estimation

In certain application scenarios, data-driven models are primarily used for state estimation. In contrast, physical models provide physical constraints and explanations to ensure that the predictions made by data-driven models are physically reasonable and reliable. This strategy not only maximizes the advantages of data-driven models in learning complex features but also ensures the physical consistency of the prediction results, effectively reducing the risks of overfitting and bias. Kim et al. [118] proposed multi-PINN for modeling and predicting thermal runaways in LIBs. Kim et al. [118] proposed multi-PINN for modeling and predicting thermal runaways in LIBs. Multi-PINN incorporates multi-physical equations, such as energy balance equations, reaction kinetics, and boundary conditions, into the loss function of the neural network, establishing a supervisory mechanism for physical information. Multi-PINN consists of two sub-networks: one for predicting temperature distribution and another for predicting the spatiotemporal distribution of reactant concentrations. By coupling multiple physical fields, the model shares inputs and optimization objectives during training, ensuring it can accurately describe complex chemical reactions. Najera-Flores et al. [125] improved the BNN by utilizing the physical property of the monotonic decrease of LIB discharge capacity as a constraint. They also combined several innovative approaches, including using neural differential operators, designing architectures similar to deep operator networks, and constructing a multi-loss function comprising reconstruction loss, physical constraint loss, numerical consistency loss, and complexity loss. By implementing physical constraints through automatic differentiation, the model enhances the accuracy of RUL predictions and quantifies prediction uncertainties. Wang et al. [126] proposed a degradation modeling method based on PINN, treating the degradation of LIBs as a process influenced by time and operating conditions. The study combined empirical degradation models with state-space equations to describe the battery's degradation behavior, introducing partial differential equations as degradation equations to ensure that the degradation predictions align with physical laws. The model's loss function includes data loss, partial differential equation loss, and monotonicity loss, ensuring physical consistency and prediction accuracy during training.

(d) Parallel prediction at the model level

In addition to the three serial or unidirectional strategies mentioned above, physical and data-driven models can run in parallel, independently making predictions. These are then integrated through a fusion mechanism (such as a KF or weighted averaging). This strategy effectively combines the advantages of both physical and data-driven models, resulting in a more comprehensive and accurate state estimation. Liu et al. [121] combined the AR model with the ECM. They used a multiscale H∞ filter algorithm to estimate joint states across multiple time scales. The AR-MM model describes the overall characteristics of the battery pack, integrating data-driven AR models with ECM feature information. The Rint-DM describes the deviation between the individual cells and the overall performance of the battery pack, reflecting the inconsistency between individual cells via internal resistance differences (ΔR0). The multiscale H∞ filter algorithm is used to jointly estimate the SOC and capacity across different time scales, thus improving the precision and reliability of state estimation. Zhang et al. [122] proposed a framework for joint estimation of the SOH and SOC. Initially, a GRU network is used for one-step prediction of SOH, and the prediction results from the GRU are then used as the observation equation. The Ampere-hour integration is used as the state equation, and a PF is employed to estimate SOC. The framework sets checkpoints after several charge–discharge cycles and corrects SOH estimation using incremental capacity peak features to further reduce SOH prediction errors. This forms a closed-loop control, reducing the accumulation of prediction errors. Kouhestani et al. [127] proposed a data-driven prognosis method for fault detection and lifespan prediction in LIBs. The method introduces local conservativeness by minimizing curvature around each observation point, avoiding explicit dependence on the physical

model's conservation equations. The method does not require offline training and only utilizes in situ measurement data, implementing predictions by minimizing local curvature within the neighborhood of the observation points. This improves the flexibility and real-time capabilities of fault detection.

6. Conclusions

This paper reviews the latest research progress in LIB state estimation, focusing on techniques based on physical models, data-driven models, and hybrid models. Physical models estimate the state by simulating the battery's electrochemical, thermodynamic, and other internal processes. Common models include ECM, thermal, and aging models, which can provide precise behavior predictions under ideal conditions but have limitations under complex operating environments and battery aging. In contrast, data-driven models rely on big data and machine learning algorithms to estimate the state by extracting features from historical data. These methods can handle complex nonlinear behaviors without physical meaning and require high-quality, abundant data. Hybrid models combine the advantages of physical and data-driven models, incorporating prior knowledge from physical models with the adaptability of data-driven methods. This combination improves estimation accuracy while enhancing system robustness and adaptability. Specifically, hybrid models adopt multi-physical fusion, multi-data-driven fusion, and multi-physical-data-driven fusion approaches, which combine microscopic electrochemical reactions with macroscopic electrical characteristics, as well as complementary aspects at the network structure, model architecture, and functional module levels, achieving more accurate state estimation in complex environments. Looking ahead, with the continuous advancement of multi-model fusion technologies, combining the strengths of both physical and data-driven models will be key to improving LIB state estimation accuracy, particularly when dealing with complex operating conditions, different battery chemistries, and new battery technologies (such as solid-state and lithium–sulfur batteries). Hybrid models will demonstrate stronger adaptability and accuracy. As machine learning algorithms (such as reinforcement learning and transfer learning) are applied in BMS, future hybrid models will handle more variable operating conditions and enable smarter real-time estimation. Furthermore, future BMS will become more intelligent and reliable, with the ability to adaptively select the most appropriate model, enhancing battery lifecycle management efficiency and driving the widespread adoption of electric vehicles and energy storage systems.

Funding: The work is supported by the National Natural Science Foundation of China (No. 62173281, 52377217, U23A20651), Sichuan Science and Technology Program (No. 24NSFSC0024, 23ZDYF0734, 23NSFSC1436), Dazhou City School Cooperation Project (No. DZXQHZ006), Technopole Talent Summit Project (No. KJCRCFH08), and Robert Gordon University.

Conflicts of Interest: The authors declare no conflict of interest.

References

1. Khan, F.N.U.; Rasul, M.G.; Sayem, A.; Mandal, N.K. Design and optimization of lithium-ion battery as an efficient energy storage device for electric vehicles: A comprehensive review. *J. Energy Storage* **2023**, *71*, 108033–108065. [CrossRef]
2. Nyamathulla, S.; Dhanamjayulu, C. A review of battery energy storage systems and advanced battery management system for different applications: Challenges and recommendations. *J. Energy Storage* **2024**, *86*, 111179–111205. [CrossRef]
3. Sesidhar, D.; Badachi, C.; Green, I.I.R.C. A review on data-driven SOC estimation with Li-Ion batteries: Implementation methods & future aspirations. *J. Energy Storage* **2023**, *72*, 108420–108442.
4. Peng, S.; Zhu, J.; Wu, T.; Tang, A.; Kan, J.; Pecht, M. SOH early prediction of Lithium-ion batteries based on voltage interval selection and features fusion. *Energy* **2024**, *308*, 132993–133007. [CrossRef]
5. Chen, W.; Chen, J.; Chen, Z.; Lin, H.; Chen, S.; Chen, J.; Chen, H.; Chen, W. A Data-Driven Online SOP Estimation Method for Lithium-ion Capacitors. In Proceedings of the 2023 5th Asia Energy and Electrical Engineering Symposium (AEEES), Chengdu, China, 23–26 March 2023; IEEE: Piscataway, NJ, USA, 2023; pp. 1130–1135.
6. Koseoglou, M.; Tsioumas, E.; Panagiotidis, I.; Papagiannis, D.; Jabbour, N.; Mademlis, C. A lithium-ion battery equivalent circuit model based on a hybrid parametrization approach. *J. Energy Storage* **2023**, *73*, 109051–109058. [CrossRef]

7. Tao, J.; Wang, S.; Cao, W.; Cui, Y.; Fernandez, C.; Guerrero, J.M. Innovative multiscale fusion-antinoise extended long short-term memory neural network modeling for high precision state of health estimation of lithium-ion batteries. *Energy* **2024**, *312*, 133541–133559. [CrossRef]
8. Jin, H.; Gao, Z.; Zuo, Z.; Zhang, Z.; Wang, Y.; Zhang, A. A combined model-based and data-driven fault diagnosis scheme for lithium-ion batteries. *IEEE Trans. Ind. Electron.* **2023**, *71*, 6274–6284. [CrossRef]
9. Wang, Y.; Zhang, X.; Liu, K.; Wei, Z.; Hu, X.; Tang, X.; Chen, Z. System identification and state estimation of a reduced-order electrochemical model for lithium-ion batteries. *Etransportation* **2023**, *18*, 100295–100307. [CrossRef]
10. Tang, A.; Huang, Y.; Liu, S.; Yu, Q.; Shen, W.; Xiong, R. A novel lithium-ion battery state of charge estimation method based on the fusion of neural network and equivalent circuit models. *Appl. Energy* **2023**, *348*, 121578–121589. [CrossRef]
11. Wang, D.; Yang, Y.; Gu, T. A hierarchical adaptive extended Kalman filter algorithm for lithium-ion battery state of charge estimation. *J. Energy Storage* **2023**, *62*, 106831–106842. [CrossRef]
12. Al-Greer, M.; Bashir, I. Physics-based model informed smooth particle filter for remaining useful life prediction of lithium-ion battery. *Measurement* **2023**, *214*, 112838–112851.
13. Babu, P.S. VI Enhanced SOC estimation of lithium ion batteries with RealTime data using machine learning algorithms. *Sci. Rep.* **2024**, *14*, 16036–16052.
14. Peng, J.; Meng, J.; Wu, J.; Deng, Z.; Lin, M.; Mao, S.; Stroe, D.-I. A comprehensive overview and comparison of parameter benchmark methods for lithium-ion battery application. *J. Energy Storage* **2023**, *71*, 108197–108223. [CrossRef]
15. Kim, E.; Kim, M.; Kim, J.; Kim, J.; Park, J.-H.; Kim, K.-T.; Park, J.H.; Kim, T.; Min, K. Data-driven methods for predicting the state of health, state of charge, and remaining useful life of li-ion batteries: A comprehensive review. *Int. J. Precis. Eng. Manuf.* **2023**, *24*, 1281–1304. [CrossRef]
16. Sutanto, E.; Astawa, P.E.; Fahmi, F.; Hamid, M.I.; Yazid, M.; Shalannanda, W.; Aziz, M. Lithium-ion battery state-of-charge estimation from the voltage discharge profile using gradient vector and support vector machine. *Energies* **2023**, *16*, 1083. [CrossRef]
17. Gotz, J.D.; Galvão, J.R.; Corrêa, F.C.; Badin, A.A.; Siqueira, H.V.; Viana, E.R.; Converti, A.; Borsato, M. Random Forest-Based Grouping for Accurate SOH Estimation in Second-Life Batteries. *Vehicles* **2024**, *6*, 799–813. [CrossRef]
18. Pan, R.; Liu, T.; Huang, W.; Wang, Y.; Yang, D.; Chen, J. State of health estimation for lithium-ion batteries based on two-stage features extraction and gradient boosting decision tree. *Energy* **2023**, *285*, 129460–129474. [CrossRef]
19. Ge, D.; Jin, G.; Wang, J.; Zhang, Z. A novel data-driven IBA-ELM model for SOH/SOC estimation of lithium-ion batteries. *Energy* **2024**, *305*, 132395–132410. [CrossRef]
20. Xu, H.; Wu, L.; Xiong, S.; Li, W.; Garg, A.; Gao, L. An improved CNN-LSTM model-based state-of-health estimation approach for lithium-ion batteries. *Energy* **2023**, *276*, 127585–127595. [CrossRef]
21. Tao, J.; Wang, S.; Cao, W.; Zhang, M.; Bobobee, E.D. An improved log-cosine variation slime mold-simplified gated recurrent neural network for the high-precision state of charge estimation of lithium-ion batteries. *J. Energy Storage* **2024**, *94*, 112412–112424. [CrossRef]
22. Cai, Y.; Li, W.; Zahid, T.; Zheng, C.; Zhang, Q.; Xu, K. Early prediction of remaining useful life for lithium-ion batteries based on CEEMDAN-transformer-DNN hybrid model. *Heliyon* **2023**, *9*, e17754. [CrossRef] [PubMed]
23. Obregon, J.; Han, Y.-R.; Ho, C.W.; Mouraliraman, D.; Lee, C.W.; Jung, J.-Y. Convolutional autoencoder-based SOH estimation of lithium-ion batteries using electrochemical impedance spectroscopy. *J. Energy Storage* **2023**, *60*, 106680–106690. [CrossRef]
24. Ye, M.; Wang, Q.; Yan, L.; Wei, M.; Lian, G.; Zhao, K.; Zhu, W. Enhanced robust capacity estimation of lithium-ion batteries with unlabeled dataset and semi-supervised machine learning. *Expert Syst. Appl.* **2024**, *238*, 121892–121904. [CrossRef]
25. Khaleghi, S.; Hosen, M.S.; Van Mierlo, J.; Berecibar, M. Towards machine-learning driven prognostics and health management of Li-ion batteries. *A Compr. Rev. Renew. Sustain. Energy Rev.* **2024**, *192*, 114224–114254. [CrossRef]
26. He, W.; Li, Z.; Liu, T.; Liu, Z.; Guo, X.; Du, J.; Li, X.; Sun, P.; Ming, W. Research progress and application of deep learning in remaining useful life, state of health and battery thermal management of lithium batteries. *J. Energy Storage* **2023**, *70*, 107868–107903. [CrossRef]
27. Tian, J.; Chen, C.; Shen, W.; Sun, F.; Xiong, R. Deep learning framework for lithium-ion battery state of charge estimation: Recent advances and future perspectives. *Energy Storage Mater.* **2023**, *61*, 102883–102899. [CrossRef]
28. Zeng, Y.; Li, Y.; Yang, T. State of charge estimation for lithium-ion battery based on unscented Kalman filter and long short-term memory neural network. *Batteries* **2023**, *9*, 358. [CrossRef]
29. Zhang, L.; Xia, B.; Zhang, F. Adaptive fault detection for lithium-ion battery combining physical model-based observer and BiLSTMNN learning approach. *J. Energy Storage* **2024**, *91*, 112067–112085. [CrossRef]
30. Meng, H.; Hu, M.; Kong, Z.; Niu, Y.; Liang, J.; Nie, Z.; Xing, J. Risk analysis of lithium-ion battery accidents based on physics-informed data-driven Bayesian networks. *Reliab. Eng. Syst. Saf.* **2024**, *251*, 110294–110308. [CrossRef]
31. Nicodemo, N.; Di Rienzo, R.; Lagnoni, M.; Bertei, A.; Baronti, F. Estimation of lithium-ion battery electrochemical properties from equivalent circuit model parameters using machine learning. *J. Energy Storage* **2024**, *99*, 113257–113266. [CrossRef]
32. Zhang, Y.; Wik, T.; Bergström, J.; Zou, C. State of health estimation for lithium-ion batteries under arbitrary usage using data-driven multimodel fusion. *IEEE Trans. Transp. Electrif.* **2023**, *10*, 1494–1507. [CrossRef]
33. Ji, C.; Dai, J.; Zhai, C.; Wang, J.; Tian, Y.; Sun, W. A Review on Lithium-Ion Battery Modeling from Mechanism-Based and Data-Driven Perspectives. *Processes* **2024**, *12*, 1871. [CrossRef]
34. Zhao, J.; Zhu, Y.; Zhang, B.; Liu, M.; Wang, J.; Liu, C.; Hao, X. Review of state estimation and remaining useful life prediction methods for lithium–ion batteries. *Sustainability* **2023**, *15*, 5014. [CrossRef]

35. Ghaeminezhad, N.; Ouyang, Q.; Wei, J.; Xue, Y.; Wang, Z. Review on state of charge estimation techniques of lithium-ion batteries: A control-oriented approach. *J. Energy Storage* **2023**, *72*, 108707–108731. [CrossRef]
36. Zhou, L.; Lai, X.; Li, B.; Yao, Y.; Yuan, M.; Weng, J.; Zheng, Y. State estimation models of lithium-ion batteries for battery management system: Status, challenges, and future trends. *Batteries* **2023**, *9*, 131. [CrossRef]
37. Tao, J.; Wang, S.; Cao, W.; Takyi-Aninakwa, P.; Fernandez, C.; Guerrero, J.M. A comprehensive review of state-of-charge and state-of-health estimation for lithium-ion battery energy storage systems. *Ionics* **2024**, *30*, 5903–5927. [CrossRef]
38. Liu, Y.; Wang, L.; Li, D.; Wang, K. State-of-health estimation of lithium-ion batteries based on electrochemical impedance spectroscopy: A review. *Prot. Control Mod. Power Syst.* **2023**, *8*, 1–17. [CrossRef]
39. Urquizo, J.; Singh, P. A review of health estimation methods for Lithium-ion batteries in Electric Vehicles and their relevance for Battery Energy Storage Systems. *J. Energy Storage* **2023**, *73*, 109194–109205. [CrossRef]
40. Liu, F.; Yu, D.; Shao, C.; Liu, X.; Su, W. A review of multi-state joint estimation for lithium-ion battery: Research status and suggestions. *J. Energy Storage* **2023**, *73*, 109071–109091. [CrossRef]
41. Sun, X.; Zhang, Y.; Zhang, Y.; Wang, L.; Wang, K. Summary of health-state estimation of lithium-ion batteries based on electrochemical impedance spectroscopy. *Energies* **2023**, *16*, 5682. [CrossRef]
42. Ren, Z.; Du, C. A review of machine learning state-of-charge and state-of-health estimation algorithms for lithium-ion batteries. *Energy Rep.* **2023**, *9*, 2993–3021. [CrossRef]
43. Martí-Florences, M.; Cecilia, A.; Costa-Castelló, R. Modelling and Estimation in Lithium-Ion Batteries: A Literature Review. *Energies* **2023**, *16*, 6846. [CrossRef]
44. Ouyang, T.; Wang, C.; Xu, P.; Ye, J.; Liu, B. Prognostics and health management of lithium-ion batteries based on modeling techniques and Bayesian approaches: A review. *Sustain. Energy Technol. Assess.* **2023**, *55*, 102915–102929. [CrossRef]
45. Yang, B.; Qian, Y.; Li, Q.; Chen, Q.; Wu, J.; Luo, E.; Xie, R.; Zheng, R.; Yan, Y.; Su, S.; et al. Critical summary and perspectives on state-of-health of lithium-ion battery. *Renew. Sustain. Energy Rev.* **2024**, *190*, 114077–114104. [CrossRef]
46. Chen, G.; Peng, W.; Yang, F. An LSTM-SA model for SOC estimation of lithium-ion batteries under various temperatures and aging levels. *J. Energy Storage* **2024**, *84*, 110906. [CrossRef]
47. Takyi-Aninakwa, P.; Wang, S.; Liu, G.; Bage, A.N.; Masahudu, F.; Guerrero, J.M. An enhanced lithium-ion battery state-of-charge estimation method using long short-term memory with an adaptive state update filter incorporating battery parameters. *Eng. Appl. Artif. Intell.* **2024**, *132*, 107946. [CrossRef]
48. Fan, X.; Feng, H.; Yun, X.; Wang, C.; Zhang, X. SOC estimation for lithium-ion battery based on AGA-optimized AUKF. *J. Energy Storage* **2024**, *75*, 109689. [CrossRef]
49. Li, F.; Zuo, W.; Zhou, K.; Li, Q.; Huang, Y.; Zhang, G. State-of-charge estimation of lithium-ion battery based on second order resistor-capacitance circuit-PSO-TCN model. *Energy* **2024**, *289*, 130025. [CrossRef]
50. Chen, H.; Liu, F.; Hou, H.; Shen, X. Estimation of fractional SOC for lithium batteries based on OCV hysteretic characteristics. *Ionics* **2024**, *30*, 2627–2641. [CrossRef]
51. Barcellona, S.; Codecasa, L.; Colnago, S. Inverse Open Circuit Voltage Curve Model for $LiCoO_2$ Battery at Different Temperatures. *Energies* **2024**, *17*, 5137. [CrossRef]
52. Vignesh, S.; Che, H.S.; Selvaraj, J.; Tey, K.S.; Lee, J.W.; Shareef, H.; Errouissi, R. State of Health (SoH) estimation methods for second life lithium-ion battery—Review and challenges. *Appl. Energy* **2024**, *369*, 123542.
53. Dini, P.; Colicelli, A.; Saponara, S. Review on modeling and soc/soh estimation of batteries for automotive applications. *Batteries* **2024**, *10*, 34. [CrossRef]
54. Gao, Z.; Xie, H.; Yang, X.; Wang, W.; Liu, Y.; Xu, Y.; Ma, B.; Liu, X.; Chen, S. SOH estimation method for lithium-ion batteries under low temperature conditions with nonlinear correction. *J. Energy Storage* **2024**, *75*, 109690. [CrossRef]
55. Demirci, O.; Taskin, S.; Schaltz, E.; Demirci, B.A. Review of battery state estimation methods for electric vehicles-Part II: SOH estimation. *J. Energy Storage* **2024**, *96*, 112703. [CrossRef]
56. Xie, Y.; Wang, S.; Zhang, G.; Takyi-Aninakwa, P.; Fernandez, C.; Blaabjerg, F. A review of data-driven whole-life state of health prediction for lithium-ion batteries: Data preprocessing, aging characteristics, algorithms, and future challenges. *J. Energy Chem.* **2024**, *97*, 630–649. [CrossRef]
57. Su, L.; Xu, Y.; Dong, Z. State-of-health estimation of lithium-ion batteries: A comprehensive literature review from cell to pack levels. *Energy Convers. Econ.* **2024**, *5*, 224–242. [CrossRef]
58. Shrivastava, P.; Naidu, P.A.; Sharma, S.; Panigrahi, B.K.; Garg, A. Review on technological advancement of lithium-ion battery states estimation methods for electric vehicle applications. *J. Energy Storage* **2023**, *64*, 107159. [CrossRef]
59. Raoofi, T.; Yildiz, M. Comprehensive review of battery state estimation strategies using machine learning for battery Management Systems of Aircraft Propulsion Batteries. *J. Energy Storage* **2023**, *59*, 106486. [CrossRef]
60. Dai, H.; Jiang, B.; Hu, X.; Lin, X.; Wei, X.; Pecht, M. Advanced battery management strategies for a sustainable energy future: Multilayer design concepts and research trends. *Renew. Sustain. Energy Rev.* **2021**, *138*, 110480. [CrossRef]
61. Guo, R.; Shen, W. A review of equivalent circuit model based online state of power estimation for lithium-ion batteries in electric vehicles. *Vehicles* **2021**, *4*, 1–29. [CrossRef]
62. Rojas, O.E.; Khan, M.A. A review on electrical and mechanical performance parameters in lithium-ion battery packs. *J. Clean. Prod.* **2022**, *378*, 134381. [CrossRef]

63. Naseri, F.; Karimi, S.; Farjah, E.; Schaltz, E. Supercapacitor management system: A comprehensive review of modeling, estimation, balancing, and protection techniques. *Renew. Sustain. Energy Rev.* **2022**, *155*, 111913. [CrossRef]
64. Mukherjee, S.; Chowdhury, K. State of charge estimation techniques for battery management system used in electric vehicles: A review. *Energy Systems.* **2023**, 1–44. [CrossRef]
65. Zhang, S.; Zhang, X. A novel low-complexity state-of-energy estimation method for series-connected lithium-ion battery pack based on "representative cell" selection and operating mode division. *J. Power Sources* **2022**, *518*, 230732. [CrossRef]
66. Zhang, S.; Zhang, X. A novel non-experiment-based reconstruction method for the relationship between open-circuit-voltage and state-of-charge/state-of-energy of lithium-ion battery. *Electrochim. Acta* **2022**, *403*, 139637. [CrossRef]
67. Ren, Y.; Jin, C.; Fang, S.; Yang, L.; Wu, Z.; Wang, Z.; Peng, R.; Gao, K. A comprehensive review of key technologies for enhancing the reliability of lithium-ion power batteries. *Energies* **2023**, *16*, 6144. [CrossRef]
68. Shan, C.; Chin, C.S.; Mohan, V.; Zhang, C. Review of Various Machine Learning Approaches for Predicting Parameters of Lithium-Ion Batteries in Electric Vehicles. *Batteries* **2024**, *10*, 181. [CrossRef]
69. Uzair, M.; Abbas, G.; Hosain, S. Characteristics of battery management systems of electric vehicles with consideration of the active and passive cell balancing process. *World Electr. Veh. J.* **2021**, *12*, 120. [CrossRef]
70. Huang, H.; Bian, C.; Wu, M.; An, D.; Yang, S. A novel integrated SOC–SOH estimation framework for whole-life-cycle lithium-ion batteries. *Energy* **2024**, *288*, 129801–129810. [CrossRef]
71. Mo, D.; Wang, S.; Fan, Y.; Takyi-Aninakwa, P.; Zhang, M.; Wang, Y.; Fernandez, C. Enhanced multi-constraint dung beetle optimization-kernel extreme learning machine for lithium-ion battery state of health estimation with adaptive enhancement ability. *Energy* **2024**, *307*, 132723–132738. [CrossRef]
72. Ma, C.; Wu, C.; Wang, L.; Chen, X.; Liu, L.; Wu, Y.; Ye, J. A Review of Parameter Identification and State of Power Estimation Methods for Lithium-Ion Batteries. *Processes* **2024**, *12*, 2166. [CrossRef]
73. Li, J.; Wang, S.; Chen, L.; Wang, Y.; Zhou, H.; Guerrero, J.M. Adaptive Kalman filter and self-designed early stopping strategy optimized convolutional neural network for state of energy estimation of lithium-ion battery in complex temperature environment. *J. Energy Storage* **2024**, *83*, 110750–110762. [CrossRef]
74. Liu, H.; Li, Y.; Luo, L.; Zhang, C. A lithium-ion battery capacity and rul prediction fusion method based on decomposition strategy and GRU. *Batteries* **2023**, *9*, 323. [CrossRef]
75. Ramezani-al, M.R.; Moodi, M. A novel combined online method for SOC estimation of a Li-Ion battery with practical and industrial considerations. *J. Energy Storage* **2023**, *67*, 107605–107618. [CrossRef]
76. Rodríguez-Iturriaga, P.; Anseán, D.; Rodríguez-Bolívar, S.; González, M.; Viera, J.C.; López-Villanueva, J.A. A physics-based fractional-order equivalent circuit model for time and frequency-domain applications in lithium-ion batteries. *J. Energy Storage* **2023**, *64*, 107150–107164. [CrossRef]
77. Li, R.; Li, K.; Liu, P.; Zhang, X. Research on Multi-Time Scale SOP Estimation of Lithium–Ion Battery Based on H∞ Filter. *Batteries* **2023**, *9*, 191. [CrossRef]
78. An, F.; Zhang, W.; Sun, B.; Jiang, J.; Fan, X. A novel state-of-energy simplified estimation method for lithium-ion battery pack based on prediction and representative cells. *J. Energy Storage* **2023**, *63*, 107083–107096. [CrossRef]
79. Li, D.; Liu, X.; Cheng, Z. The co-estimation of states for lithium-ion batteries based on segment data. *J. Energy Storage* **2023**, *62*, 106787–106798. [CrossRef]
80. Wang, J.; Meng, J.; Peng, Q.; Liu, T.; Zeng, X.; Chen, G.; Li, Y. Lithium-ion battery state-of-charge estimation using electrochemical model with sensitive parameters adjustment. *Batteries* **2023**, *9*, 180. [CrossRef]
81. Feng, Y.; Xue, C.; Han, F.; Cao, Z.; Yang, R.J. State-of-Charge and State-of-Health Estimation in Li-Ion Batteries Using Cascade Electrochemical Model-Based Sliding-Mode Observers. *Batteries* **2024**, *10*, 290. [CrossRef]
82. Hashemzadeh, P.; Désilets, M.; Lacroix, M. Online state estimation of Li-ion batteries using continuous-discrete nonlinear Kalman filters based on a nonlinear simplified electrochemical model. *Electrochim. Acta* **2024**, *481*, 143953–143969. [CrossRef]
83. Yu, Z.; Tian, Y.; Li, B. A simulation study of Li-ion batteries based on a modified P2D model. *J. Power Sources* **2024**, *618*, 234376–234393. [CrossRef]
84. Yu, H.; Zhang, L.; Wang, W.; Yang, K.; Zhang, Z.; Liang, X.; Chen, S.; Yang, S.; Li, J.; Liu, X. Lithium-ion battery multi-scale modeling coupled with simplified electrochemical model and kinetic Monte Carlo model. *iScience* **2023**, *26*, 107661. [CrossRef]
85. Chen, H.; Zhang, T.; Chen, H.; Gao, Q. Thermoelectric coupling model construction of 21,700 cylindrical ternary lithium batteries under wide temperature range environment. *J. Therm. Anal. Calorim.* **2024**, *149*, 12071–12082. [CrossRef]
86. Zeng, J.; Wang, S.; Cao, W.; Zhou, Y.; Fernandez, C.; Guerrero, J.M. Battery asynchronous fractional-order thermoelectric coupling modeling and state of charge estimation based on frequency characteristic separation at low temperatures. *Energy* **2024**, *307*, 132730–132746. [CrossRef]
87. Xu, Z.; Zhang, C.; Sun, B.; Liu, S. The electric-thermal coupling simulation and state estimation of lithium-ion battery. *J. Energy Storage* **2023**, *58*, 106431–106446. [CrossRef]
88. Liu, W.; Teh, J.; Alharbi, B.; Yang, G.; Wang, B.; Meng, D.; Shi, J.; AlKassem, A.; Aljabr, A.; Alshammari, N. An electric-thermal coupling modeling method for lithium-ion battery using the state of charge normalization calculation method. *J. Energy Storage* **2023**, *72*, 108724–108738. [CrossRef]
89. Gayathri, R.; Husna, M.A.U.; Poojasri, R.; Sutha, S.; Pappa, N.; Vijayakarthick, M. Hybrid Electro-Thermal model based optimal charging of Lithium-ion Battery using MOGA for Enhanced State-of-Health. *IFAC-PapersOnLine* **2024**, *57*, 173–178. [CrossRef]

90. Li, Y.; Wang, L.; Feng, Y.; Liao, C.; Yang, J. An online state-of-health estimation method for lithium-ion battery based on linear parameter-varying modeling framework. *Energy* **2024**, *298*, 131277–131291. [CrossRef]
91. Fang, D.; Wu, W.; Li, J.; Yuan, W.; Liu, T.; Dai, C.; Wang, Z.; Zhao, M. Performance simulation method and state of health estimation for lithium-ion batteries based on aging-effect coupling model. *Green Energy Intell. Transp.* **2023**, *2*, 100082–100095. [CrossRef]
92. Zhang, Q.; Wang, D.; Schaltz, E.; Stroe, D.-I.; Gismero, A.; Yang, B. Lithium-ion battery calendar aging mechanism analysis and impedance-based State-of-Health estimation method. *J. Energy Storage* **2023**, *64*, 107029–107042. [CrossRef]
93. Hofmann, T.; Li, J.; Hamar, J.; Erhard, S.; Schmidt, J.P. The ΔQ-method: State of health and degradation mode estimation for lithium-ion batteries using a mechanistic model with relaxed voltage points. *J. Power Sources* **2024**, *596*, 234107–234121. [CrossRef]
94. Wang, G.; Cui, N.; Li, C.; Cui, Z.; Yuan, H. A state-of-health estimation method based on incremental capacity analysis for Li-ion battery considering charging/discharging rate. *J. Energy Storage* **2023**, *73*, 109010–109020. [CrossRef]
95. Xiong, W.; Xu, G.; Li, Y.; Zhang, F.; Ye, P.; Li, B. Early prediction of lithium-ion battery cycle life based on voltage-capacity discharge curves. *J. Energy Storage* **2023**, *62*, 106790–106798. [CrossRef]
96. Wang, Y.; Chen, X.; Li, C.; Yu, Y.; Zhou, G.; Wang, C.; Zhao, W. Temperature prediction of lithium-ion battery based on artificial neural network model. *Appl. Therm. Eng.* **2023**, *228*, 120482–120496. [CrossRef]
97. Wang, Z.; Liu, N.; Chen, C.; Guo, Y. Adaptive self-attention LSTM for RUL prediction of lithium-ion batteries. *Inf. Sci.* **2023**, *635*, 398–413. [CrossRef]
98. Zhang, C.; Wang, H.; Wu, L. Life prediction model for lithium-ion battery considering fast-charging protocol. *Energy* **2023**, *263*, 126109–126121. [CrossRef]
99. Qin, H.; Fan, X.; Fan, Y.; Wang, R.; Shang, Q.; Zhang, D. A Computationally Efficient Approach for the State-of-Health Estimation of Lithium-Ion Batteries. *Energies* **2023**, *16*, 5414. [CrossRef]
100. Hai, N.; Wang, S.; Huang, Q.; Xie, Y.; Fernandez, C. Improved K-means clustering-genetic backpropagation modeling for online state-of-charge estimation of lithium-ion batteries adaptive to low-temperature conditions. *J. Energy Storage* **2024**, *99*, 113399–113415. [CrossRef]
101. Fei, Z.; Huang, Z.; Zhang, X. Voltage and temperature information ensembled probabilistic battery health evaluation via deep Gaussian mixture density network. *J. Energy Storage* **2023**, *73*, 108587–108600. [CrossRef]
102. Wu, M.; Zhong, Y.; Wu, J.; Wang, Y.; Wang, L. State of health estimation of the lithium-ion power battery based on the principal component analysis-particle swarm optimization-back propagation neural network. *Energy* **2023**, *283*, 129061–129069.
103. Sudarshan, M.; Serov, A.; Jones, C.; Ayalasomayajula, S.M.; García, R.E.; Tomar, V. Data-driven autoencoder neural network for onboard BMS Lithium-ion battery degradation prediction. *J. Energy Storage* **2024**, *82*, 110575–110583. [CrossRef]
104. Zeng, Y.; Meng, J.; Peng, J.; Feng, F.; Yang, F. State of health estimation of lithium-ion battery considering sensor uncertainty. *J. Energy Storage* **2023**, *72*, 108667–108676. [CrossRef]
105. Shi, H.; Wang, S.; Huang, Q.; Fernandez, C.; Liang, J.; Zhang, M.; Qi, C.; Wang, L. Improved electric-thermal-aging multi-physics domain coupling modeling and identification decoupling of complex kinetic processes based on timescale quantification in lithium-ion batteries. *Appl. Energy* **2024**, *353*, 122174–122195. [CrossRef]
106. Xi, R.; Mu, Z.; Ma, Z.; Jin, W.; Ma, H.; Liu, K.; Li, J.; Yu, M.; Jin, D.; Cheng, F. Lifetime prediction of rechargeable lithium-ion battery using multi-physics and multiscale model. *J. Power Sources* **2024**, *608*, 234622–234631. [CrossRef]
107. Wang, Y.; Li, J.; Guo, S.; Zhao, M.; Cui, W.; Li, L.; Zhao, L.; Wang, Z. A method of lithium-ion battery failure diagnosis based on parameter boundaries of heterogeneous multi-physics aging model. *J. Power Sources* **2023**, *576*, 233235–233244.
108. Zhou, B.; Fan, G.; Wang, Y.; Liu, Y.; Chen, S.; Sun, Z.; Meng, C.; Yang, J.; Zhang, X. Life-extending optimal charging for lithium-ion batteries based on a multi-physics model and model predictive control. *Appl. Energy* **2024**, *361*, 122918–122942. [CrossRef]
109. Li, J.; Ye, M.; Ma, X.; Wang, Q.; Wang, Y. SOC estimation and fault diagnosis framework of battery based on multi-model fusion modeling. *J. Energy Storage* **2023**, *65*, 107296–107308. [CrossRef]
110. Sun, C.; Gao, M.; Cai, H.; Xu, F.; Zhu, C. Data-driven state-of-charge estimation of a lithium-ion battery pack in electric vehicles based on real-world driving data. *J. Energy Storage* **2024**, *101*, 113986–114000. [CrossRef]
111. Zhang, Y.; Wik, T.; Bergström, J.; Zou, C. Practical battery State of Health estimation using data-driven multi-model fusion. *IFAC-PapersOnLine* **2023**, *56*, 3776–3781. [CrossRef]
112. Xiong, X.; Wang, Y.; Li, K.; Chen, Z. State of health estimation for lithium-ion batteries using Gaussian process regression-based data reconstruction method during random charging process. *J. Energy Storage* **2023**, *72*, 108390–108402. [CrossRef]
113. Xia, Z.; Wu, Y. A hybrid network of NARX and DS-attention applied for the state estimation of lithium-ion batteries. *Int. J. Electrochem. Sci.* **2024**, *19*, 100632–100640. [CrossRef]
114. Wang, C.; Zhang, X.; Yun, X.; Meng, X.; Fan, X. Robust state-of-charge estimation method for lithium-ion batteries based on the fusion of time series relevance vector machine and filter algorithm. *Energy* **2023**, *285*, 129466–129478. [CrossRef]
115. Pang, H.; Wu, L.; Liu, J.; Liu, X.; Liu, K. Physics-informed neural network approach for heat generation rate estimation of lithium-ion battery under various driving conditions. *J. Energy Chem.* **2023**, *78*, 1–12. [CrossRef]
116. Mao, L.; Hu, Q.; Zhao, J.; Yu, X. State-of-charge of lithium-ion battery based on equivalent circuit model–Relevance vector machine fusion model considering varying ambient temperatures. *Measurement* **2023**, *221*, 113487–113499. [CrossRef]
117. Dai Nguyen, C.; Bae, S.J. Equivalent circuit simulated deep network architecture and transfer learning for remaining useful life prediction of lithium-ion batteries. *J. Energy Storage* **2023**, *71*, 108042–108055. [CrossRef]

118. Kim, S.W.; Kwak, E.; Kim, J.-H.; Oh, K.-Y.; Lee, S. Modeling and prediction of lithium-ion battery thermal runaway via multiphysics-informed neural network. *J. Energy Storage* **2023**, *60*, 106654–106669. [CrossRef]
119. Das Goswami, B.R.; Mastrogiorgio, M.; Ragone, M.; Jabbari, V.; Shahbazian-Yassar, R.; Mashayek, F.; Yurkiv, V. A combined multiphysics modeling and deep learning framework to predict thermal runaway in cylindrical Li-ion batteries. *J. Power Sources* **2024**, *595*, 234065–234077. [CrossRef]
120. Wang, C.; Li, R.; Cao, Y.; Li, M. A hybrid model for state of charge estimation of lithium-ion batteries utilizing improved adaptive extended Kalman filter and long short-term memory neural network. *J. Power Sources* **2024**, *620*, 235272–235285. [CrossRef]
121. Liu, F.; Yu, D.; Su, W.; Bu, F. Multi-state joint estimation of series battery pack based on multi-model fusion. *Electrochim. Acta* **2023**, *443*, 141964–141980. [CrossRef]
122. Zhang, Y.; Gu, P.; Duan, B.; Zhang, C. A hybrid data-driven method optimized by physical rules for online state collaborative estimation of lithium-ion batteries. *Energy* **2024**, *301*, 131710–131724. [CrossRef]
123. Wu, J.; Meng, J.; Lin, M.; Wang, W.; Wu, J.; Stroe, D.-I. Lithium-ion battery state of health estimation using a hybrid model with electrochemical impedance spectroscopy. *Reliab. Eng. Syst. Saf.* **2024**, *252*, 110450–110466. [CrossRef]
124. Murawwat, S.; Gulzar, M.M.; Alzahrani, A.; Hafeez, G.; Khan, F.A.; Abed, A.M. State of charge estimation and error analysis of lithium-ion batteries for electric vehicles using Kalman filter and deep neural network. *J. Energy Storage* **2023**, *72*, 108039–108060.
125. Najera-Flores, D.A.; Hu, Z.; Chadha, M.; Todd, M.D. A physics-constrained Bayesian neural network for battery remaining useful life prediction. *Appl. Math. Model.* **2023**, *122*, 42–59. [CrossRef]
126. Wang, F.; Zhai, Z.; Zhao, Z.; Di, Y.; Chen, X. Physics-informed neural network for lithium-ion battery degradation stable modeling and prognosis. *Nat. Commun.* **2024**, *15*, 4332–4343. [CrossRef]
127. Kouhestani, H.S.; Liu, L.; Wang, R.; Chandra, A. Data-driven prognosis of failure detection and prediction of lithium-ion batteries. *J. Energy Storage* **2023**, *70*, 108045–108056. [CrossRef]